AD-A101 398 SOIL CONSERVATION SERVICE OXFORD MS SEDIMENTATION LAB F/G 20/4
STREAM CHANNEL STABILITY. APPENDIX M. LARGE-SCALE MODEL STUDY O--ETC(U)
APR 81 J C WILLIS

UNCLASSIFIED NL

END
DATE FILMED
7 81
DTIC

LEVEL III

STREAM CHANNEL STABILITY

APPENDIX M

LARGE SCALE MODEL STUDY OF BED MATERIAL TRANSPORT

Project Objective 4

by

J. C. Willis

USDA Sedimentation Laboratory
Oxford, Mississippi

April 1981

Prepared for
US Army Corps of Engineers, Vicksburg District
Vicksburg, Mississippi

Under
Section 32 Program, Work Unit 7

STREAM CHANNEL STABILITY,
APPENDIX M

LARGE-SCALE MODEL STUDY OF BED-MATERIAL TRANSPORT

Project Objective 4

by

Joe C. Willis 1/

USDA Sedimentation Laboratory

Oxford, Mississippi

April 1981

Prepared for

US Army Corps of Engineers, Vicksburg District
Vicksburg, Mississippi

Under

Section 32 Program, Work Unit 7

1/ Research Hydraulic Engineer, Sediment Transport and Deposition Unit, USDA Sedimentation Laboratory, Oxford, MS.

Preface

In a stable alluvial channel, no net erosion or deposition of sediment occurs on the average. The sediment supply rate from upstream is balanced by capacity of the flow to transport the bed material. Any successful channel design must maintain this equilibrium or establish it for channel reaches that are not stable. Design relationships between the bed material transport capacity and the hydraulic variables of flow are based primarily on data from relatively small test channels. Reliable data for equilibrium transport of bed material by flows over about twenty cfs are not adequate to insure that data from small flumes can be extrapolated to prototype designs.

An investigation was conducted in the 250-ft long test channel at the USDA Sedimentation Laboratory to obtain additional data on equilibrium transport by flows up to 150 cfs. Data on the transport rates, flow friction factors, and statistical properties of the bed forms were obtained. The results are presented as basic variable correlations with the controlled variables of the experiments, depth and discharge, along with attempts to generalize the relationships by similitude principles.

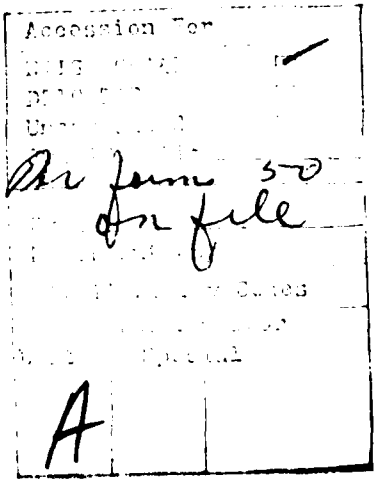

Table of Contents

List of Tables

List of Figures

CONVERSION FACTORS, U.S. CUSTOMARY TO METRIC (SI) AND METRIC (SI) TO U.S. CUSTOMARY UNITS OF MEASUREMENT[1/]

Units of measurement used in this report can be converted as follows:

To convert	To	Multiply by
mils (mil)	micron (μm)	25.4
inches (in)	millimeters (mm)	25.4
feet (ft)	meters (m)	0.305
yards (yd)	meters (m)	0.914
miles (miles)	kilometers (km)	1.61
inches per hour (in/hr)	millimeters per hour (mm/hr)	25.4
feet per second (ft/sec)	meters per second (m/sec)	0.305
square inches (sq in)	square millimeters (mm^2)	645.
square feet (sq ft)	square meters (m^2)	0.093
square yards (sq yd)	square meters (m^2)	0.836
square miles (sq miles)	square kilometers (km^2)	2.59
acres (acre)	hectares (ha)	0.405
acres (acre)	square meters (m^2)	4,050.
cubic inches (cu in)	cubic millimeters (mm^3)	16,400.
cubic feet (cu ft)	cubic meters (m^3)	0.0283
cubic yards (cu yd)	cubic meters (m^3)	0.765
cubic feet per second (cfs)	cubic meters per second (cms)	0.0283
pounds (lb) mass	grams (g)	454.
pounds (lb) mass	kilograms (kg)	0.453
tons (ton) mass	kilograms (kg)	907.
pounds force (lbf)	newtons (N)	4.45
kilogram force (kgf)	newtons (N)	9.81
foot pound force (ft lbf)	joules (J)	1.36
pounds force per square foot (psf)	pascals (Pa)	47.9
pounds force per square inch (psi)	kilopascals (kPa)	6.89
pounds mass per square foot (lb/sq ft)	kilograms per square meter (kg/m^2)	4.88
U.S. gallons (gal)	liters (L)	3.79
quart (qt)	liters (L)	0.946
acre-feet (acre-ft)	cubic meters (m^3)	1,230.
degrees (angular)	radians (rad)	0.0175
degrees Fahrenheit (F)	degrees Celsius (C)[2/]	0.555

2/ To obtain Celsius (C) readings from Fahrenheit (F) readings, use the following formula: C = 0.555 (F-32).

Metric (SI) to U.S. Customary

To convert	To	Multiply by
micron (μm)	mils (mil)	0.0394
millimeters (mm)	inches (in)	0.0394
meters (m)	feet (ft)	3.28
meters (m)	yards (yd)	1.09
kilometers (km)	miles (miles)	0.621
millimeters per hour (mm/hr)	inches per hour (in/hr)	0.0394
meters per second (m/sec)	feet per second (ft/sec)	3.28
square millimeters (mm^2)	square inches (sq in)	0.00155
square meters (m^2)	square feet (sq ft)	10.8
square meters (m^2)	square yards (sq yd)	1.20
square kilometers (km^2)	square miles (sq miles)	0.386
hectares (ha)	acres (acre)	2.47
square meters (m^2)	acres (acre)	0.000247
cubic millimeters (mm^3)	cubic inches (cu in)	0.0000610
cubic meters (m^3)	cubic feet (cu ft)	35.3
cubic meters (m^3)	cubic yards (cu yd)	1.31
cubic meters per second (cms)	cubic feet per second (cfs)	35.3
grams (g)	pounds (lb) mass	0.00220
kilograms (kg)	pounds (lb) mass	2.20
kilograms (kg)	tons (ton) mass	0.00110
newtons (N)	pounds force (lbf)	0.225
newtons (N)	kilogram force (kgf)	0.102
joules (J)	foot pound force (ft lbf)	0.738
pascals (Pa)	pounds force per square foot (psf)	0.0209
kilopascals (kPa)	pounds force per square inch (psi)	0.145
kilograms per square meter (kg/m^2)	pounds mass per square foot lb/sq ft)	0.205
liters (L)	U.S. gallons (gal)	0.264
liters (L)	quart (qt)	1.06
cubic meters (m^3)	acre-feet (acre-ft)	0.000811
radians (rad)	degrees (angular)	57.3
degrees Celsius (C)	degrees Fahrenheit (F)3/	1.8

1/ All conversion factors to three significant digits.

3/ To obtain Fahrenheit (F) readings from Celsius (C) readings, use the following formula: $F = 1.8C + 32$.

Notation

a	- reference level above the bed surface
C	- average sediment concentration
c	- local sediment concentration
$C_i, C_{iT},$ C_{iI}, C_{iF}	- individual pump/record concentrations
$C(f)$	- Co-spectral density
D	- grain diameter similitude number
d_{50}	- median particle size
e	- base of natural logarithms
E_s	- sediment diffusivity
f	- frequency, spatial or temporal
F	- Froude number
f_f	- Darcy-Weisbach friction factor
f'	- part of friction factor due to grain roughness
f''	- part of friction factor due to form resistance
g	- gravity constant
G_d	- volumetric dune load
$h_{iT}, h_{iI},$ h_{iF}	- pressure heads from individual flow meters/records
K_i	- flow meter calibration factors
N_R	- Reynolds number
q	- flow discharge per unit of channel width
Q_i	- individual pump discharges
$Q(f)$	- quadrature spectral density
S_e	- energy gradient
s'	- part of energy gradient due to grain roughness
s''	- part of energy gradient due to form resistance
$S(f)$	- spectral density
$SC(f)$	- cross-spectral density
V	- mean flow velocity
$V(f)$	- migration velocity of bed frequency components
V_d	- average dune velocity
Δx	- ultrasonic probe spacing
$\theta(f)$	- phase angles

ν - kinematic viscosity

π - mathematical symbol denoting ~ 3.14159

ρ_s - sediment density

ρ_w - water density

σ - dimensionless standard deviation (normalized to unity)

σ_b - bed standard deviation

σ_c - concentration standard deviation

σ_L - spatial standard deviation of the bed surface

σ_t - temporal standard deviation of the bed surface

Υ - time shift placing two bed records "in phase"

1 INTRODUCTION

Sediment transport processes of alluvial streams are important aspects of channel stability. Channel instabilities result from erosion of sediment from or deposition on the stream's bed or banks. This erosion or deposition occurs because of an imbalance between the capacity of the flow to transport sediment and the sediment supply rates from upstream reaches. Any rectification of the channel system must balance the transport capacity of a new set of hydraulic variables and the sediment supply rates to the channel.

Relationships between the transport capacity and the hydraulic variables are necessary if a successful design is to be developed. Valid relationships have been quite allusive. Numerous equations and calculation procedures have been proposed, but their results differ widely under similar applications. The variability of estimates may be due to a number of factors among which are the temporal and spatial variations in the flow and transport rate in field channels, difficulties of measurement of the transport rates; and the difficulty of assessing the generality of experimental relations, when the variables upon which the transport rate is considered to depend, are themselves interrelated.

To overcome the problems of unsteady flow and to facilitate measurement of the transport rates, a number of flume investigations have been conducted. Any one of these may still manifest the estimate difficulties mentioned above and some may still present nonvalid results because of an imbalance in sediment capacity and supply. However, combinations of a number of valid investigations have suggested general relationships between the transport rate and the flow variables. Unfortunately, almost all controlled flume experiments have been for fairly small flows relative to those of streams for which rectification designs are needed. Transport similarity may not exist between flows of greatly different scales, so additional experimental investigations are needed for larger, controlled flows to verify or revise the transport similitude relationships from small-scale experiments.

This study of total bed material transport in the 250-foot outdoor test channel at the USDA Sedimentation Laboratory was designed to obtain accurate measurements of the sediment load and hydraulic characteristics of the flow to test the generality of existing transport relationships. The

experiments were designed to provide not only estimates of average flow and transport properties but also temporal and spatial records of the bed forms and temporal records of the sediment transport rate. From these records time and distance scales should aid in assessing the significance of the average quantities and define measures of the bed roughness, which is important in establishing the regime of a channel.

The statistical analysis of the sediment load and bed forms is considered to be an important aspect of this investigation because the expected long periods of significant deviations from the mean may result in short-term means that may deviate significantly from the long-term mean. Also, the selective erosion and deposition of dunes induces variations in the sediment transport rate, so that the pertubations in the concentration and bed-form records should be coupled. A comparison of the results from large-scale experiments with comparable data from smaller flumes should aid in assessing the generality of transport relationships.

The overall goal of the investigation is the development of transport relationships that can be used to estimate the average transport rates in existing, equilibrium reaches of stream channels and to provide the hydraulic variables for redesign of an unstable reach. The results should also provide an estimate of natural deviations from the average that may be accomodated by different flow rates in the channel.

Over some long time period a stable stream may be considered to have adjusted its geometry in response to the valley slope so that the transport capacity for both water and sediment equals the runoff and erosion quantities delivered to it from the watershed. Not just one set of "design" variables but a spectrum of different flows, sediment quantities, and different sediment sizes are delivered to the channel. These complexities are compounded by natural statistical pertutations of constant flow, and even more so by local instabilities within nonuniform channel reaches wherein local disturbances and high erosivities, such as on the outside of a bend, may interrupt the transport balance. Some distance downstream may be required to re-establish the transport balance and for fine sediments no balance may ever be achieved.

The question may then be asked whether a design can be accomplished in view of the deviations in the mean transport rate from the average, upon which the design is proposed to be based. The bed material of a stream

provides the degrees of freedom whereby the range of flows and transport rates, as well as pertubations from the average, may be accomodated. A stream can adjust to small deviations between the sediment supply and capacity by depositing sediment on or eroding it from the stream bed. The sediment storage is quite limited but the stream bed imparts another degree of freedom to the transport processes through variation in bed roughness. Bed roughness can change appreciably and it will have an appreciable influence on the hydraulic resistance and, consequently, the velocity and depth of flow for a given flow rate. When the sediment concentration is low, the bed forms may be large with high flow resistance giving a greater depth, lower velocity, and a lower transport capacity. When the concentration is high, the bed forms tend to be obliterated leaving a rather smooth bed with low hydraulic resistance and a shallower depth, higher velocity, and higher transport capacity.

The preceeding adjustments occur naturally in a stream channel and are predicated on the assumption that the blanket of bed material is preserved. If the blanket of sand or gravel is removed, not only are the transport adjustments that rely on this blanket of material no longer present, but also the underlying alluvium is exposed to the erosive action of the flow. If the boundary material is erodible, an unstable channel is likely to develop. Thus design criteria should be predicated on preservation of the bed material through equilibrium transport of the sediment fractions represented therein.

2 LITERATURE REVIEW

2.1 SEDIMENT DISCHARGE RELATION

Numerous formulas and procedures have been proposed for estimating the transport rates of sediment since Dubois proposed his classical equation in 1879 (Brown, 1950). These relationships have varied in analytical complexity from extremely complex calculation procedures typlified by the Einstein Bed-Load Functions (Einstein, 1950) and other methods based thereon (Modified Einstein, Toffelete, etc.) to experimental correlations of the basic variables typlified by the method of Colby (1964). Irrespective of the theoretical complexity, at some point in the load derivations the state of the art becomes inadequate and experimental data must be used to bridge the non-existant theory. Hence, from the standpoint of strictly a predictive tool, the degree of analytical complexity may offer no real advantage or promise of improved prediction.

A treatment of the various transport relationships is considered beyond the scope of this report in view of the availability of two excellent review articles on the subject (ASCE Task Committee 1971, Shulitz and Hill 1968). In these articles, the reliability of the various transport formula are questioned. Great disparity is shown between calculations of sediment rating curves for actual stream channels. But then there are other streams for which any one formula would likely give good results. Certainly each formula or correlation must be considered to define reliably the data set upon which it was based.

The disparity between sediment load calculations and the apparent absence of a generally applicable computation method have led some researchers to conclude that the problem is indeterminent. If there is a determinent relationship between the amount of sediment that streams can carry and the hydraulic variables of their flows, it is quite elusive. Either the analyses have failed to adequately account for the pertinent variables, or the data have been biased by nongeneral influences and measurement deficiencies.

The quest for general transport relationships has led researchers to be selective of stream reaches and to resort to experiments in laboratory flumes. The mechanism of sediment suspension, which is probably the best understood of the transport processes, vividly illustrates the qualitative

influence that secondary flows associated with nonuniform flow geometry, can have on the transport rate. Measurement problems over alluvial beds negate reliable load measurements, except those associated with some natural or artificial structure, wherein the entire sediment load is suspended. For these measurements to be useful in developing load predictions they must be associated with the hydraulics of a uniform channel reach. Unsteady flows further complicate the problem of obtaining reliable field data.

Flume experiments, while permitting steady flows in apparently uniform reaches, are still not immune to nongeneralities. They will almost always incorporate discharges lower than those of significance in natural channels. Are the results of these small-scaled experiments applicable to large river channels? Sediment generally enters the flumes in some non-equilibrium distribution at the upper end of the flume. Is the flume channel long enough for the load and flow to reach equilibrium over an adequate flume length to determine the pertinent hydraulic variables? (Willis, et al., 1972). Were experimental techniques used that may have altered the apparent relationships between transport rates and flow variables? An example might be artificial planing of the sand bed, followed by insufficient time for equilibrium bed form and slope adjustments (Gilbert, 1914). Even experiments with good, reliable data may often give correlations that are non-general because of imposed relationships between the variables that have been chosen to be treated as independent (Willis, 1980). The flow rating curve of natural channels is an example, in that relationships between all the hydraulic variables are imposed. Even if the transport rate should not depend on one of these variables, an apparent correlation will exist by virtue of the mutual correlation with true controlling variables.

Numerous flume investigations have been conducted to provide measurements of sediment transport rates under controlled conditions. A survey of the available flume data was made by Willis and Coleman (1969) with the questions of the preceeding section as a guide. Enough data, that were considered to include reliable flow and transport rate measurements under equilibrium conditions, were compiled to define a unified correlation. Unfortunately, the discharges and channel systems were much smaller than most natural streams for which design relationships are needed. The need

for reliable data for larger flow systems serves as one of the primary justifications of the current investigation.

The problem of developing general, equilibrium transport relationships involves not only providing an adequate data base, but also specificating a sufficient set of unique independent variables, and formulating the relationships needed for design criteria. Certainly authors do not agree on the set of independent variables to use in the formulation. Some select shear stress as the major controlling flow variable. Others prefer mean velocity; still others use flow discharge; and yet others stream power. If we select an analysis like that of Colby (1964) which shows that the equilibrium transport rate of bed material is a function of only mean velocity and flow depth for given sediment properties and temperature, the conclusion is that only two hydraulic variables are necessary for a general relationship. This appears as an over-simplified analysis in view of the complexities of some methods. However, the sediment rating curves calculated by the ASCE Task Committee (1971) for the Colorado and Niobrara Rivers show that the Colby method does as well if not better than other methods in predicting observed transport data.

Further justification of the 2H (two hydraulic variables) approach can be obtained by considering the variables that may be controlled in a sand-bed, laboratory flume. In a closed system with tailwater control, the depth and discharge may be controlled. The slope of this type flume may also be adjustable, but if an incorrect slope is set, scour and erosion will occur in adjusting to a different equilibrium slope. Other flumes will have the sediment feed rate and discharge as the primary controls. Auxiliary controls may also be available, but they can only hasten the development of equilibrium conditions.

The premise here, although without universal acceptance, (Williams, 1970) is that only two variables can be controlled in addition to sediment and fluid properties for equilibrium flow and transport. Hence, only two variables need to be considered as independent. All other variables react or adjust in response to these selected independent controls. However, an extension of this premise is that we are not bound by the physical controls in selecting the independent variables for analysis purposes. Any two basic variables may be treated as independent no matter what other controls were actually adjusted to achieve these variables. The discharge and

sediment feed rate may be adjusted to give the desired velocity and depth, or slope and discharge can give the same results provided that flow and transport processes are allowed to reach equilibrium before the final velocity and depth are measured. Likewise, even though the sediment load (feed rate) may be controlled, it may be considered as a means to arrive at a desired velocity and depth of flow, and, consequently, as a dependent variable-dependent on the resulting velocity and depth.

Whereas the preceeding discussion has emphasized the use of velocity and depth as independent variables, any two unique variables could be chosen as independent. Other researchers prefer combinations of the basic variables in the form of shear stress and stream power per unit of bed area (Yang, 1973). Such combinations are equally valid provided that at least two unique combinations are retained in the analysis, and may be consistent with the authors' theoretical visualizations of the transport processes. For the current investigation, retention of basic variables in the analyses is preferable.

An extension of the basic variable analysis of Colby was made by Willis and Coleman (1969) based on basic hydraulic principles - the equations of motion for a sediment water mixture, and the principle of dimensional homogeny. In the equations of motion, the mean flow velocity and flow depth were logical units of measure for the variable velocities and lengths, respectively, of the flow system. The volumetric sediment concentration became a logical measure of the variability of the fluid density. In terms of the dimensionless variables, coefficients of the various terms included three dimensionless expressions of the sediment load and flow variables. These are the density corrected sediment concentration, sediment concentration, $\frac{\rho_s - \rho_w}{\rho_w} C$; the Froude number, $V/\sqrt{gy_t}$; and the Reynolds number, Vy_t/ν. Here ρ_s and ρ_w denote densities of sediment and water, respectively, C is the average sediment concentration, V is the mean flow velocity, y_t the flow depth, and ν the kinematic viscosity.

When the coefficients of the dimensionless differential equation and the boundary conditions on the dimensionless variables are the same, the solution of the equation in terms of the dimensionless variables must also be the same. The coefficients of the dimensionless equation then specify

transport or flow similitude, and relationships between these coefficients then specify similitude regimes for the flow/transport process. Hence, the density corrected sediment concentraton may be considered to depend on the Froude number and Reynolds number.

Between the different flume investigations, sediment size was a controlled variable. Although the median sediment size, d_{50}, does not enter the equations of motion directly, it certainly influences the flow and boundary roughness. Therefore it is treated as a boundary condition parameter with an appropriate dimensionless expression, $\frac{g^{1/3}d_{50}}{\nu^{2/3}}$. Thus the density corrected concentration must also be considered to be dependent on this parameter as well as the two dimensionless hydraulic parameters.

One of the fortuitous aspects of fluid mechanics is that the effects of the Reynolds number (viscous forces) diminish in importance at high Reynolds numbers. The same phenomenon seems to hold true for transport processes, in that no Reynolds number influence on the concentration is discernible from compilation of flume data. However, for tests at small Reynolds numbers under non-equilibrium conditions, a definite Reynolds number dependency was noted (Willis, 1971). But for experiments in flumes with Reynolds numbers greater than about 10^4, the sediment concentration correlates fairly well with Froude number alone for a given sediment size. Considering the usual disappearance of Reynolds number influences at high Reynolds numbers, we would expect the transport similitude relationships to apply at still higher Reynolds numbers. However one of the unstated assumptions of the method is that depth characterizes all length scales of the system. A question then arises concerning the length scales of the bed geometry. Without experiments at greater depths, only conjectures can be offered for boundary influences which strongly influence the flow and transport processes.

2.2 HYDRAULIC RELATIONSHIPS

Basic variable and similitude correlations should serve as reliable design criteria, however they assume that hydraulic variables are known when, in fact, they may be completely unknown. What channel geometry and

slope are needed to give the desired Froude number and sediment concentration? Probably most of the complexities of the Einstein Bed-Load Function arise from attempts to calculate flow hydraulics from a given channel slope and geometry.

From arguments of the preceeding section, all aspects of the flow should be uniquely specified by the Reynolds number and Froude number of the flow for constant sediment and fluid properties. This would include the slope, and from the definition of the Darcy-Weisbach resistance coefficient, f_f

$$f_f = \frac{8gy_t S_e}{V^2} = \frac{8S_e}{F^2} \tag{1}$$

this resistance factor would also be uniquely specified. Here y_t is the flow depth, S_e is the energy gradient, V is the flow velocity, and F is the Froude Number.

A number of different methods of estimating channel hydraulic relationships were presented by the ASCE Task Committee (1971). In view of the excellent review and the review presented in Appendix Chapter L, only a summary of one particular procedure will be treated here.

Because it is closely related to similitude analysis of the transport processes, the method of Alam, Lovera, and Kennedy (ASCE Task Committee, 1971) will be considered in some detail here. In their procedure the friction factor and slope (energy gradient) are separated into that part, f', due to the bed material roughness (grain roughness) and that part due to the bed forms, f", (form roughness), ie;

$$f_f = f' + f" \tag{2}$$

$$S_e = s' + s" \tag{3}$$

where s' and s" denote portions of the energy gradient contributed by grain and form resistance, respectively. The form resistance part is postulated from dimensional analysis to depend on two similitude parameters:

$$f" = f" \left(\frac{V}{\sqrt{gd_{50}}}, \frac{d_{50}}{y_t}\right) \tag{4}$$

or

$$f'' = f''\ (F\ ,\ \frac{d_{50}}{y_t}) \tag{5}$$

where side wall effects are assumed to be neglible and the depth y_t has been substituted for the bed hydraulic radius.

The grain resistance part is postulated to depend on the Reynolds number, N_R, and the relative grain diameter:

$$f' = f'\ (N_R\ ,\ \frac{d_{50}}{y_t}) \tag{6}$$

From the Lovera and Kennedy diagram, for a given f' value, y_t/d_{50} is strongly dependent on N_R. In fact, the following approximate relation holds,

$$\frac{y_t}{d_{50}} \propto (N_R)^{2/3} \tag{7}$$

with the constant of proportionality depending on f'.

Then,

$$f' = f'\ (\frac{y_t}{d_{50}}(N_R)^{-2/3}) = f'\ (\frac{y_t}{d_{50}}\ \frac{v^{2/3}}{V^{2/3}Y_t^{2/3}}\ ) \tag{8}$$

$$= f'\ (\frac{y_t^{1/3}}{V^{2/3}}\ .\ \frac{v^{2/3}}{d_{50}})$$

Note that $\frac{y_t^{1/3}}{V^{2/3}} = 1/F^{2/3}\ g^{1/3}$, so

$$f' = f'\ (F^{2/3}\ .\ \frac{g^{1/3}d_{50}}{v^{2/3}}) \tag{9}$$

equation (9) then includes the same similitude numbers used in the analysis of the sediment transport processes.

The occurrence of d_{50}/y_t in equation (5) along with the Froude number still requires some Reynolds number dependency on f", since

$$y_t = (N_R/F)^{2/3} \; g^{1/3}/v^{2/3} \qquad (10)$$

However, if f' can be treated as independent of N_R, a reappearance of N_R dependency on the form resistance factor, in view of the high relative roughness of the bed forms, would seem unreasonable. If f" is independent of Reynolds number, the ratio d_{50}/y_t should be replaced by $g^{1/3} \; d_{50}/v^{2/3}$ in equation (5).

A considerable amount of discussion is present in the literature concerning the relative merits of dividing the resistance between grain and form resistance. Einstein and Barbarossa divide the hydraulic radius or depth while the above analysis divides the slope. If the above derivations based on the Alam, Lovera, and Kennedy (ASCE Task Committee, 1971) method prove to be experimentally consistent, the division process becomes unimportant since both parts are functions of the same variables.

Although specification of a more reliable resistance factor diagram is considered beyond the scope of this investigation, complete neglect of hydraulic relationships would be unreasonable. The transport processes generate the form resistance of the bed and these as well as the grain resistance contribute through the flow hydraulics to influence the transport processes themselves. The preceeding discussion is offered to assess the generality of transport relationships; to show that the similitude analysis may or may not give the same results for small-scaled and large-scaled investigations since transport and resistance have been suggested to depend on different similitude numbers.

Experimental relationships between the basic variables may serve as valid design criteria, however, they really give little insight into the actual mechanics of sediment transportation. Even though the similitude analysis is shown to be consistent with the equations of motion, these equations only serve as a means to logically organize the variables into dimensionless groups. To obtain a better understanding of transport mechanics that may permit a refinement of the models, a more detailed investigation than just measurement of the gross variables is necessary.

Primarily the drag forces of the flow cause a sediment particle to roll along the bed of a channel. A particle that has been swept up into the body of the flow moves along at about the velocity of the surrounding

fluid imparting a small drag force. It is suspended by vertical components of turbulent eddies. This type of visualization of transport mechanics has led researchers to adopt two load distinctions, bed load and suspended load.

2.3 SUSPENDED LOAD

The suspension processes are most often treated from a diffusion viewpoint. Turbulent eddies, while imparting no net volume transfer of the sediment water mixture, will give a net upward transfer of sediment since upward velocity components carry higher concentrations than downward components. This upward diffusion process is balanced by gravitational settling thus leading to equilibrium transport.

The first mathmatical expression of this suspension balance was given by Obrien in 1933. It takes the form:

$$wc + E_s \frac{dc}{dy} = 0 \tag{11}$$

where c is the concentration, y is the distance from the bed, w is the settling velocity of the sediment particles and E_s is the diffusion coefficient. Rouse (1937) first proposed that a fluid diffusion coefficient be used to approximate E_s in response to a suggestion by Von Karman. Rouse (1939) demonstrated the validity of the equation for a constant diffusion coefficient and Vanoni (1946) experimentally verified the concept for open channel flow. Subsequent work has dealt primarily with different expressions for the diffusion coefficient (Willis, 1979; Hunt, 1954; Coleman, 1969; Zagustin, 1968).

The main problem with suspension models is that they are not applicable in the immediate vicinity of a sand bed. Hence, they can only express relative concentrations:

$$\frac{c}{c_a} = \phi \left(\frac{a}{y_t}, Y\right) \tag{12}$$

in which the lower case c's denote point concentrations and a is a small reference distance above the sand bed. No theoretically satisfactory way is known to specify c_a. In equation (11), Y denotes the various flow and sediment parameters entering the suspension-diffusion processes. In the Einstein Bed-Load Function (Einstein, 1950) a is taken as $2d_{50}$ and the

suspended load is estimated by integrating the product of concentration and velocity over the depth above this level. The reference concentration c_a is taken as the average concentration associated with the difference between total load and computed suspended load for the assumption that this difference (bed load) is transported within $2d_{50}$ of the bed.

2.4 BED LOAD

In view of the assumed dominance of drag forces on transport in the near-bed region and the breakdown of suspension theory in this region, use of a "bed load" to complete a description of transport mechanics is necessary. In fact, the Dubois equation (Brown, 1950) was developed to specifically account for this part of the transport rate. These bed load expressions generally treat the transport rate as a function of the boundary shear stress. In view of the fair correlation of <u>total</u> transport rate and shear stress, the bed load relationships are often elevated to sediment discharge formulas through experimental evaluation of their parameters.

The Einstein Bed-Load Function treats the bed load as that load transported below a depth of 2d and correlates it with a value of the shear stress associated with the grain resistance. Models that treat the bed load as a function of only part of the boundary shear stress would give different results than those using the total shear stress, provided that the two shear stresses are not directly related. Englund's (1966) resistance relationship and the interpretation presented herein of the Alam, Lovera, and Kennedy similitude graphs, indicate that form and grain resistance components shear stresses are directly related so that division of the shear stress may be unnecessary from design viewpoints.

Two main problems with bed-load formulas is that no accepted definition of bed load exists and no definite theory has evolved to conceptualize the mechanics of near-bed transport. So, how can measurements of a quantity be accomplished when it is so poorly defined?

2.5 DUNE LOAD

At low Froude numbers but with significant sediment transport, the bed of a stream deforms into a maze of roughly triangular forms known as dunes or ripples. Sediment is eroded from the upstream face of the dune and

deposited on the downstream face. Associated with this selective erosion and deposition is a definite transport quantity. Its relationship to bed load depends upon the conceptualization of the bed load. If the bed load is limited to the material that moves in essentially continuous contact with the bed, then only the material that is deposited on the lee slopes of bed forms becomes the bed load but this is identically the dune load. The term dune load will be used herein to permit other bed load conceptualizations.

Most research concerning dune load transport has dealt with a means to measure and/or compute the dune load from records of bed elevation. Estimates of the transport rate have been made from either a "tracer" technique or a "sand wave" technique. As a sand particle is eroded from an upstream dune face, it travels over the bed form(s) until it is again deposited on a lee slope. During this movement it executes a certain step length. Upon deposition it remains buried for a certain rest period until it is again exposed. The average step length divided by the average time between steps (average rest period) gives the average particle velocity. The product of this average velocity and the effective thickness of the moving layer determines the dune load by the tracer technique (Lee and Jobsen, 1974).

The erosion/deposition taking place in dunes and ripples gives the impression of downstream movement of a sand wave. Although only a thin layer of sediment is actually in motion, the apparent movement of the sand waves can be used to determine the average dune load. Stein (1965) determined the dune load from observations of the volume and migration speeds of individual dunes. The average load over a number of dunes gave the average dune load. Simons, et al. (1965) found that the load determined by this method gave a good measure of the total bed-material load for low transport rates.

An extension of the wave-migration method based on the stochastic properties of bed elevation records has been investigated by several researchers. Crickmore (1967) and Willis (1968) used dual temporal records from probes spaced a short distance apart, in the direction of the flow, to estimate the mean dune speed and effective height of the dune (effective thickness of the moving layer). (Nordin (1971) and Squarer (1970) used both spatial and temporal records to estimate the dune velocities from

spectral moment ratios. Willis (1976) extended the spectral method for dual temporal records, by computing the contribution to total dune load by discrete Fourier spectral frequencies.

Application of similitude analysis in the latter investigation showed that both the dune load and the suspended load correlated well with Froude number (sediment size was constant). Hence, for this small-scaled investigation, the use of bed-suspended load distinction was unnecessary in developing tentative predictive relationships.

3 EXPERIMENTAL APPARATUS AND PROCEDURES

3.1 TEST FACILITY

Experiments were conducted in the 250 ft. outdoor test channel at the USDA Sedimentation Laboratory to provide reliable, equilibrium data on the transport of bed material. Figure 1 presents an annotated photograph of the test channel. The test facility consists of three main compartments. These are the main test channel, flow/sediment return channel, and reservoir. At one end of the reservoir is the pump sump. A vehicle ramp at the other end provides access for vehicles.

The primary purposes of the reservoir are to provide a supply of water to fill the main test channel to the desired depth and to maintain an adequate head over the pump intakes. The return channel with a width of six feet and a bed slope of 1.4% has a greater transport capacity than the main test channel and returns the flow and sediment delivered to it, by the main channel, directly to the pumps.

The main test channel is nine feet wide with 8 ft. high sidewalls. It is 250 ft. long from a rod screen at the upper end to the tailgate. The concrete bottom is level; equilibrium slopes are achieved by adjustments of the sand bed. Flow is delivered to the test channel by three propeller-type pumps that are driven by 75-horsepower electric motors. Each pump has a nominal discharge capacity of 50 cfs giving a total capacity of 150 cfs. A bypass system is provided for two of the pumps. Each bypass will carry the full discharge of its pump so the actual flow to the test channel can be adjusted to essentially any value from 0 to 150 cfs by varying the number of operating pumps and the position of valve(s) in the bypass line(s).

Flow leaving each pump, passes through a 90° elbow which has been calibrated. The elbow is the primary flow measuring device. The axises of the elbow meters are in the vertical plane and near the top of the flow circuit. The outside or high pressure tap is at the top of the elbow where air bubbles tend to accumulate. An air trap was installed on each high pressure trap to provide a continuous water path to a pressure transducer. Provision was made to periodically withdraw air accumulation from the air traps with a vacuum system. The inside or low pressure taps are at the bottom of the elbow where sand accumulations are likely. A sand trap was

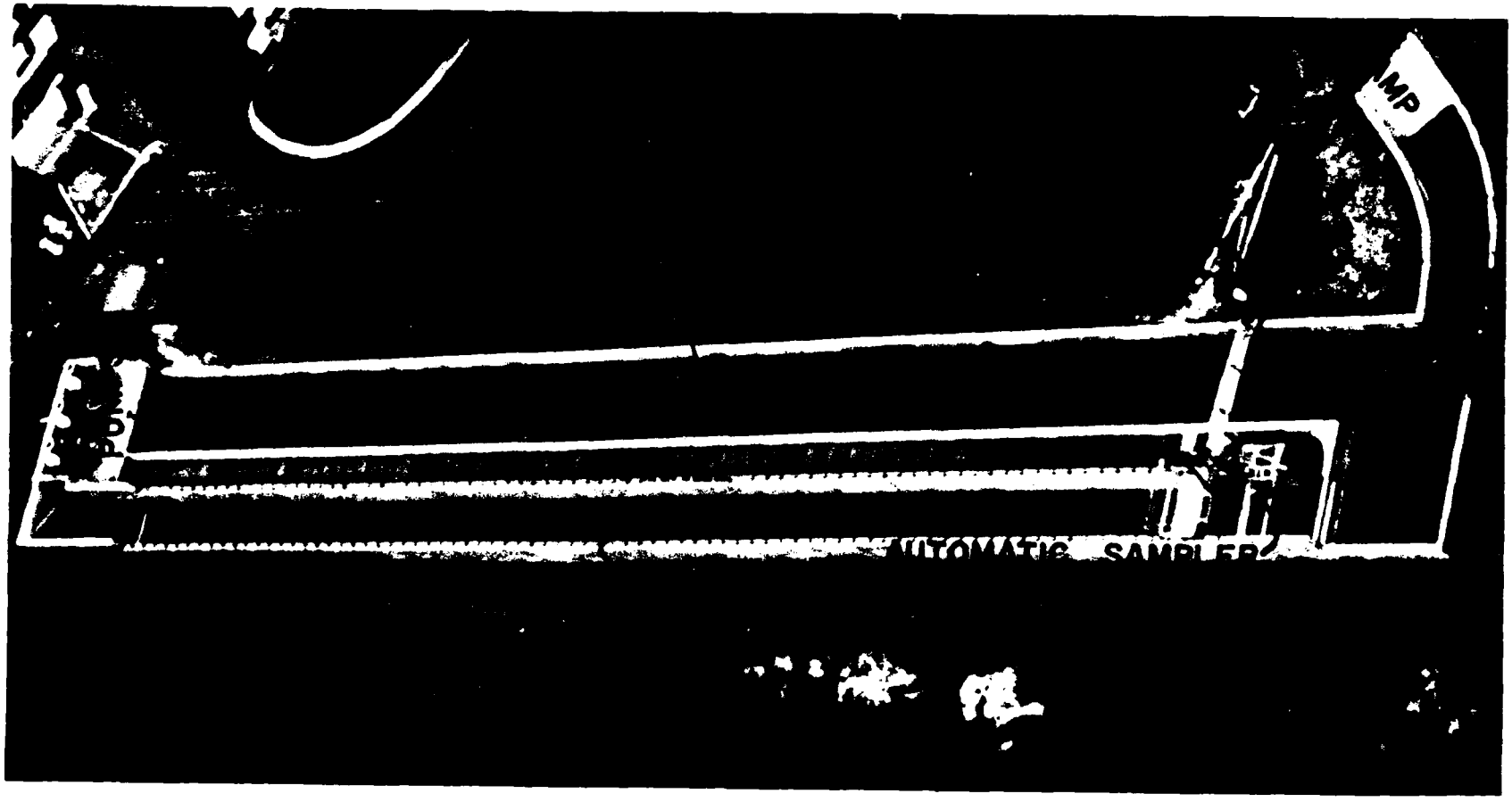

Fig. 1: 250-Ft. Test Channel

installed below the pressure transducer connection on each of these traps. The traps consist of about a two-ft. length of large-diameter vinyl tubing. As sand falls into the pressure tap, it falls past the pressure transducer connection and into the trap. A stopper at the lower end of the trap can be removed for periodic cleaning.

Flow leaves each elbow meter and discharges into the pumpbay of the channel through diverging pipe sections that lower the flow velocity. From the pumpbay it executes a 90° turn through a set of vertical miter vanes which direct a relative uniform distribution of flow across the main channel. A set of rod screens and floats further enhances the flow distribution and attenuates wave action from the flume entrance.

A roller gate at the lower end of the test channel serves as a tailwater control for the flow. An electric motor driven screw lift permits the gate to be raised to the desired level. The lift travel is adequate to raise the gate completely above the channel to permit entry of service equipment into the main channel. In its control function the gate is used as a sluice gate. The passage of both water and sediment under the gate prevents sediment accumulations from altering the tailwater control. A drop in the channel floor, immediately downstream from the tailgate, prevents backwater from the return channel and the 180° turn into the return channel, from influencing flow in the main channel.

A removable bulkhead in line with the end of the main channel separates the return channel from the reservoir at this point. Removal of the bulkhead would premit the entire flow to enter the reservoir and to be returned to the pumps through the reservoir itself. In this mode of operation, sediment would be trapped in the reservoir and virtually sediment-free water returned to the pumps. With the addition of a feed system, this mode of operation could be used with coarser sediments. In the current sand transport study, only the recirculating mode of operating was used.

The test channel was loaded with sand to an average depth of about 2.5 feet. This was an adequate depth to permit slope adjustments and to prevent the concrete bottom of the channel from being exposed in dune troughs over the test reach. A sieve analysis of the bed material gave a median diameter of 0.55 mm and a geometric standard deviation of 1.6 as shown in Figure 2. This material came from a sand quarry near Grenada,

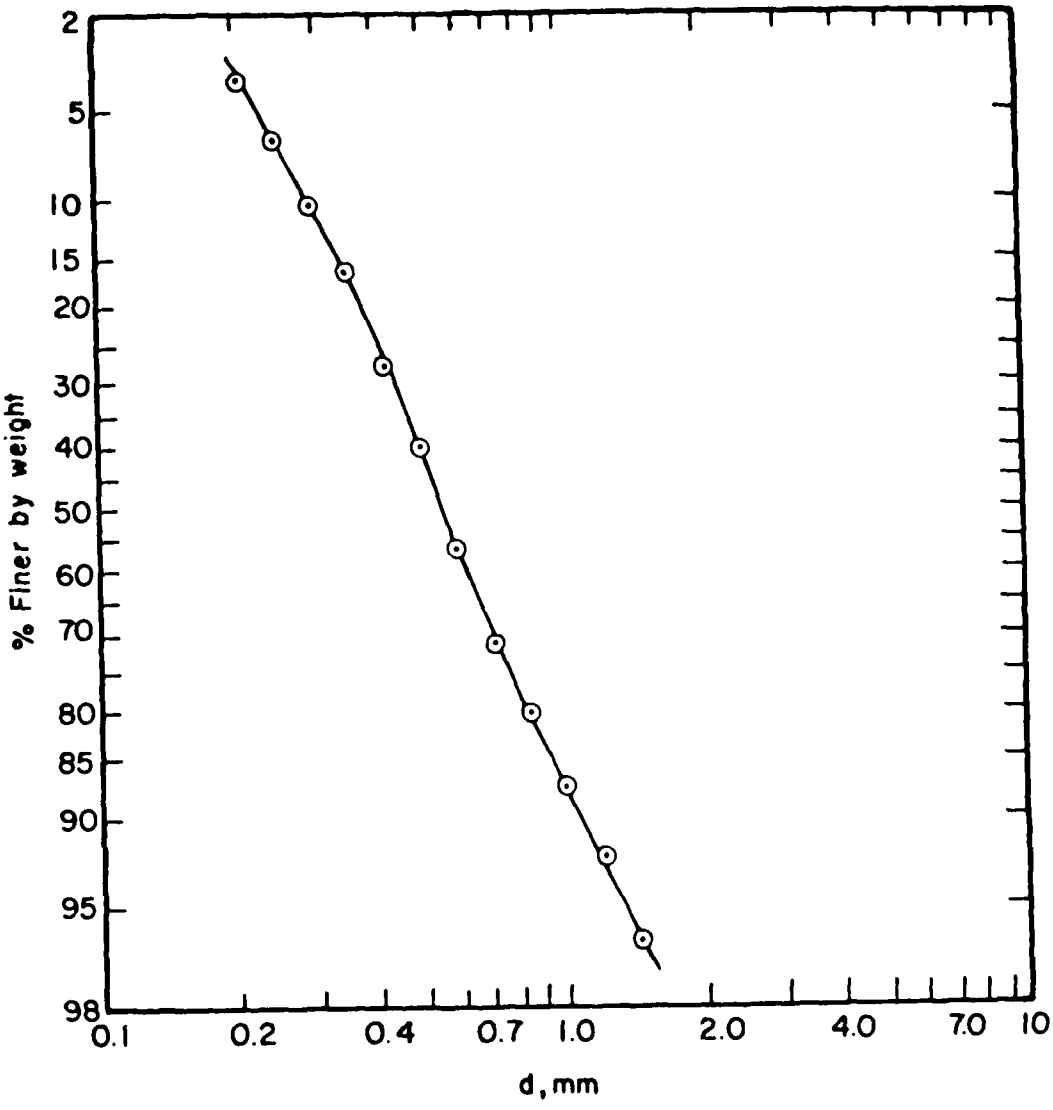

Fig. 2: Size Analysis of Bed Material

Mississippi, and should be typical of the sand fraction of the erosion products along the bluff line of the Yazoo/Mississippi River flood plain.

3.2 EXPERIMENTAL DESIGN AND INSTRUMENTATION

Experiments were designed to provide reliable data that would be applicable, not only to the gross variable type of correlation, but also to the transport-mechanics related methods. This required accurate measurement of the average transport rate along with average velocity, depth and slope under equilibrium conditions as well as measurements of suspended sediment distributions and bed form statistical properties for determination of the dune or bed load.

Two controls were available to prescribe the conditions of each test in the 250 ft. flume. These were the flow discharge and tailgate elevation. For a given discharge, the tailgate elevation could be adjusted to give the desired flow depth.

In variable-slope flumes the development of equilibrium conditions can be hastened by setting the flume slope to the expected equilibrium slope for the selected controls. However, for the outdoor test channel, no slope control is possible so adequate running time must be allowed for the sand bed to reach its own equilibrium slope in response to the imposed discharge and depth. This necessitates long equilibrium runs especially for significant changes in flow conditions.

Even under equilibrium conditions spatial and temporal variations in bed forms and local transport processes were to be expected. To ascertain the significance of the average transport rate, bed and water surface slopes, and bed form properties, information on statistical variability were needed. This necessitated almost continuous records of the sediment load or concentration, and bed and water surface elevations along the flume.

A dual channel stream monitor was available at the Sedimentation Laboratory for obtaining bed and water surface elevations by timing the travel of ultrasonic pulses from a transducer to a reflecting surface (bed or water surface) and back to the transducer. The transducers can be mounted at one position along the test channel to obtain records of the migration of bed forms along the channel or they can be moved along the flume with the flume's motorized instrument carriage to obtain spatial

records of bed and water surface elevation. The instrument is rather old so repair parts posed a problem. Failure of one channel of the instrument delayed experiments and required abbreviated experimental techniques while parts were backordered. No comparable instrumentation is currently commercially available.

The test channel was equipped with an automated sampler to collect bulk samples of the high-velocity flow under the tailgate. A modified DH-48 hand sampler driven by an electric motor and chain drive traversed the flow depth. The bottle retainer portion of the sampler is replaced with an aluminum cylinder and dumping mechanism. At the top of each traverse the sample is dumped into a trough that conveys it into a central container. The sampler moves laterally across the channel, between vertical traverses, and collects samples at about 6-inch intervals. It reverses at the walls and continues the sampling process. Concentration of sediment in the composite sample is taken to represent the total discharge concentration of sediment in the channel flow.

The concentration of the composite sample represented the average over the sampling period. Whether this represented a reasonable estimate of the long-term average could be ascertained only from continuous concentration records. To provide these records, density cells were installed on each of the pumps. A packing gland was installed in the pipe about 1 foot above the flow straightner vanes of the pump. A ½-inch diameter tube was cantilevered into the flow through the packing gland; it served as an intake nozzle for the sampler system. The sample nozzles were connected to air traps and density cells with flexible tubing. Flow from the density cells returned to the sump. Pressure from the pump forced flow through the density cell system. A tubing clamp was fabricated for the discharge side of each density cell so that the flow could be stopped and still maintain water in the cells.

The density cells consist of a vibrating U-tube through which the sample flowed and an electronic package to provide a current/voltage output proportional to the density of the sample flow. The change in output voltage from that of sediment-free water is proportional to concentration of sediment. A few changes in the density-cell system were necessary to facilitate the desired accuracy. The zero control was too coarse so a

resistor network was installed in conjunction with the existing potentiometer to permit finer adjustments. An auxiliary amplifier with a gain of about 25 was used to amplify the output voltage.

Air bubbles passing through the density cell are a problem. A hydraulic jump at the end of the return channel entrained appreciable amounts of air, so varying amounts of air entered the intake nozzles of the density cell. Small amounts of air passing through the density cell give a low voltage output indicative of low density concentrations; however, large amounts of air give maximum voltage from the density-cell/amplifier system. To eliminate air from the sample, an air trap was installed in each sample line between the intake nozzle and the density cell. The traps consist of about two foot lengths of four-inch diameter tubing with stoppers in each end. The flow enters through the top stopper and is diffused into the trap with a tee. An air-bleed tap was also installed in the top stopper. Flow leaves the trap at the bottom. A plastic funnel was cut to fit the inside of each trap. It directs the flow and sediment into the sample line and prevents sediment accumulations at the bottom of the trap.

Leaves or other foreign material sometimes plugged the intake nozzle. A backflush system was devised to sense the pressure in the air trap and to open a solenoid valve introducing a jet of water from the water supply system into a tee connection near the nozzle when the pressure dropped indicated a plugged nozzle. This reduced the frequency of manual purging required but did not completely eliminate the anomalous voltages.

To provide data on the distribution of suspended sediment throughout the flow depth, a DH-48 sampler, which had been fabricated with an intake plug valve, was used. It was mounted on the instrument carriage and used to collect samples at 0.1-0.3 foot intervals depending on the flow depth. These samples were later analyzed for total sand concentration.

Instrumentation used for the experiments developed up to eight analog voltage records. These were the two untrasonic records, three flow-meter pressure transducers, and three density cells. These analog channels were attached to eight channels of the Modcomp IV computer A-D system located in the Laboratory's computer center. The control system used to sample the data voltages permitted sampling rates up to 100 samples per second on each of the channels. During a particular experimental sequence, the voltage samples were recorded on disc and later transferred to magnetic tape for permanent storage.

The eight analog voltage channels were calibrated to permit conversion of the voltages to discharge for the pressure transducers, to probe-to-bed or water surface distance for the ultrasonic transducers, and to concentration for the density cells. Before the test channel was loaded with sand, the pressure differences across each elbow meter were related to discharge measurements in the main channel. The spatial integral of point velocity measurements made with a pitot-static tube over the flow cross section served as the discharge measurements. A number of these measurements gave the flow meter calibrations. Pressure transducers used to measure the pressure differences across the flow meters were calibrated using a test stand that enabled precise pressure differences to be imposed on the pressure transducers. These two calibrations were combined to give flow discharge proportional to the square root of the voltage from the differential pressure transducers.

The ultrasonic transducers were calibrated for several measured elevations over a plane sand bed. The transducer mounting included a point gauge and scale to facilitate precise elevation adjustments. The distance from the effective centroid of the ultrasonic transducer to the bed was proportional to the voltage. The effective centroid of the transducers was found to be 1.13 cm from their emitting surfaces. The calibrations were checked periodically and different calibration factors were used depending on the depth of flow.

The density cells were calibrated using a sand feeder to supply sediment obtained from the bed of the test channel. Sediment and water were supplied to a large funnel. A small overflow of the funnel provided a constant head and flow rate. Tubing from the funnel was connected directly to the density cell bypassing the air trap and intake nozzle from the flume pumps, but otherwise the calibration was in-place as the density cells were used in the experiments. The sample flow from each cell was collected in a one-liter Imhoff cone and the concentration determined in volumetric parts per thousand of the deposited sediment. The unit volume weight of the sediment as it deposited in the cone was found to be 1.60 gms/cc.

Contrary to the manufacturer's recommendation, the density cells were mounted with the axis of the U-tube vertical. This variation was used because the density cell responds to the spatial concentration in the U-tube. With the axis of the U-tube in the horizontal plane, sediment

would tend to settle to the bottom of the tube giving a spatial concentration much higher than the discharge concentration. With the vertical orientation, the density cells calibrated and operated satisfactorily. Also entrained sediment tends to settle out of the U-tube when the flow stops, thus permitting a reference voltage for sediment-free water to be readily obtained.

During a calibration sequence, the computer sampled the output voltage from the density cell continuously as the sand feed was started, stopped, and the feed rate changed. This gave alternating periods of sediment-free and sediment-laden flow. The change in voltage for a sediment-laden period from the average of those for the adjacent sediment-free periods was correlated with the concentration from the Imhoff cone to establish the calibrations. Several minutes were allowed following the start/stop sequences to allow the concentration in the density cell lines to stabilize.

3.3 EXPERIMENTAL PROCEDURE

Experimental procedures were developed to provide spatial records of bed and water surface elevations, reference voltage levels for sediment-free water from the density cells, temporal records of the sediment concentration from the density cells, and dual temporal records of bed elevation for equilibrium flows in the test channel. The initial phase of an experiment was the equilibrium run for a selected discharge and flow depth. For a given discharge, a number of tailgate settings were used to get different flow depths for the tests.

The flume was allowed to run for 8-16 hours before any data were collected. No significant change in bed or water surface slopes were found to occur after this length of equilibrium run. The flume could be stopped at the end of a day with minimum disturbance of the sand bed. The tailgate was lowered as the flow was progressively decreased maintaining an impoundment of water in the channel. The gate leaked slowly but an adequate depth of water was retained overnight so that the flow could be re-established with minimum disturbance. If an adequate equilibrium run had occurred the previous day, an actual data test was begun about 30 minutes after flow re-establishment. If equilibrium had not been achieved or if the impoundment had leaked too much (over weekend) an additional 8-hour equilibrium run was allowed.

During the initial 30-minute stabilization period of a data collection day, the flow meter pressure lines were purged of air, the density cell flows were checked and purged as necessary, the various electrical connections to the computer A-D systems were made, and a sample data collection made for each data channel to ascertain proper operation. Sometimes a zero drift of one or more density cells was excessive and a readjustment of the zero control(s) was necessary. This was checked and adjusted with the clamp on the density cell discharges closed.

The data collection sequence was conducted in three segments - an initial longitudinal traverse, a temporal period, and a final longitudinal traverse. Before the initial longitudinal traverse, the carriage with ultrasonic transducers was positioned about three feet upstream of the upstream end of the test reach (Station 189-18 feet from the tailgate). The upstream ultrasonic transducer was turned toward the water surface while the downstream transducer remained directed toward the bed. Flows through the density cells were clamped and the high pressure sides of each flowmeter line were clamped and the pressure transducer bypass tube opened.

The data collection program of the computer was then activated and a downstream longitudinal traverse of the flume by the carriage started. As the carriage passed station 189, Channel A of the ultrasonic meter was turned on to indicate the beginning of the spatial record. During the spatial traverse, voltages from the two ultrasonic channels, the pressure transducer, and density cells of the operating pumps were sampled. This provided reference voltage levels for zero pressure difference and sediment-free water from pressure transducers and density cells, respectively; as well as records of probe-to-bed and probe-to-watersurface distances from the two ultrasonic channels.

At times when the watersurface elevation difference over the test reach was more than one-fourth the depth, provision was made to interrupt the data sequence by turning channel A off until the ultrasonic probe could be repositioned. The carriage would be positioned a short distance upstream of the interrupt station and the drive motor restarted. Channel A would be turned on as the interrupt station was again passed. The end of the test reach (flume station 18) was also flagged in the data records by turning Channel A off.

After the initial longitudinal traverse, the upstream ultrasonic transducer was turned toward the bed and the carriage locked at flume station 18. The bypass of each pressure transducer was closed and the line from the high pressure tap of each flowmeter was opened. The discharge lines from the density cells were opened to re-establish the sample flow.

The data acquisition program was again activated to collect time voltages of bed elevation from the two ultrasonic channels (transducers separated 6 in. along the flume), pressure difference across the flow meters, and density of the sediment water mixture from the density cells. During the temporal record period, manual samples were collected over the flow depth to determine the distribution of suspended sediment in the flow. The automatic sampler was started and, after about 15 minutes to allow the sediment in the collection trough to stabilize, collection of the bulk sample was begun.

After the temporal record period, the pressure transducer and density cell connections were reset to the traverse positions. The carriage was moved to the upper end of the flume and the upstream transducer directed toward the water surrace. The spatial traverse of the flume was repeated. Completion of the final spatial record completed the test sequence. The flume tailgate and/or discharge would then be adjusted for the next test and the next equilibrium run begun.

4 DATA ANALYSIS

4.1 DATA FILTERING AND NORMALIZATION

The analysis procedures for the data from the 250 ft. test channel were designed to determine reliable measures of the basic flow and transport variables as well as statistical properties of the bed surface and sediment concentration including their means and standard deviations. Analysis of the physical samples for sediment concentration was straight forward. It involved weighing the samples to determine the total sample weight, decanting as much water as possible, drying the remaining sediment fraction and again weighing the sample. For the large total load samples (10-30 gallons of total sample) the sediment fractions were split and sieved at intervals of $(\sqrt{2})^{\frac{1}{4}}$ to obtain the size distribution for comparison with the size distribution of the bed material.

Analysis of the temporal and spatial records, as sampled by the computer, were somewhat more complex. The first step in the analysis was to delete portions of the spatial traverses that were flagged by "off" voltages on channel A and to correct the ultrasonic records for any shifts in the probe elevations that were applied near the mid point of the traverse. The portions of the density cell data and pressure transducer data corresponding to the flagged segments of channel A were also deleted to maintain the same number of data values for each channel of the traverse. The outputs of these initial analyses were continuous bed and water surface elevations relative to a fixed ultrasonic transducer elevation over the test reach.

The data records still included anomalous values. The bed and watersurface voltages included frequent unreasonably large voltages caused by a loss of echo and a few unreasonably small voltages caused by reflections from nearby suspended sediment particles. The intake nozzles of the density cells were sometimes plugged with leaves or other foreign matter and unreasonably low voltages would be recorded until the plug was removed. The pressure transducer voltages also included a few bad values during periods when air accumulations were withdrawn from the air trap on the high pressure taps of the elbow meters.

The next step in the analysis program was to obtain a plot of the raw data values for each channel with suspected anomalous voltages. A digital plotter as part of the computer hardware greatly facilitated the plotting

task. From the raw data plots upper and lower limits for reasonable data voltages and the trend of these limits over the length of record were estimated.

The third phase of the analysis procedure was to search each data channel record for data voltages outside of limits determined from the row-data plots. The previous voltage valve was substituted for any value outside the limits. Following elimination of extreme values, the mean, $\bar{x}$; variance, σ^2; and linear regression equation with slope per unit data interval, a, and intercept, b, were computed. The regression equation value, which was used to describe the trend, was subtracted from each voltage value to give a shifted data set with zero mean and no overall trend.

Checks of the voltage records showed that records without anomalous values very seldom deviated by more than 2.5 σ from the mean, or had successive values differing by as much as 0.5 σ. Six passes were then made through each channel record applying limits beginning with 5.5 σ for the maximum deviation and 3.5 σ for the maximum deviation of a voltage from the mean of its adjacent values with recomputation of σ and $\bar{x}$ after each pass. If a voltage value exceeded the maximum limit, the preceeding adjacent data voltage was substituted for it. If a value differed from the mean of its adjacent values by more than current change limit, the mean of the adjacent values was substituted for it. The limits of succeeding passes were reduced by 0.5 σ to final values of 2.5 σ and 0.5 σ. Following each pass, change in the mean was computed and the data adjusted for different regression equations. The number of data values exceeding the limit at each pass was recorded as well as the average and slope changes. The final mean data voltage and slope trends were determined as the sum of the changes from the various correction passes.

Provisions were made to output the normalized data as well as mean, standard deviation and trend parameters. Each of the residual data values were divided by the final estimate of the standard deviation to give a standardized data set with zero mean and unit standard deviation. These normalized data sets were used in additional statistical analyses to specify the probability and spectral density functions of the data records.

4.2 BASIC VARIABLE DETERMINATION

In the following analysis of the average data parameters, subscripts I and F denote the initial and final record parameters corresponding to the initial and final spatial traverses of the test reach. The subscript t denotes the temporal record values. Each of the voltage values was multiplied by the appropriate calibration factors to give quantities proportional to the probe-to-bed or watersurface distances, y_b or y_s; the pressure head, h_i; and concentration, C_i. The subscript, i, denotes a value for each pump. The subscript ℓ is used to denote either I or F.

The flow depth, y_ℓ, was determined for each spatial traverse from the ultrasonic records by

$$y_\ell = y_b + y_s + 0.199 \tag{13}$$

where y_b and y_s denote distances from the ultrasonic transducer to bed and water surface, respectively. All distances are in feet and the constant 0.199 denotes the difference in the effective levels of the ultrasonic transducers. The final estimate of the average flow depth y_t was obtained by averaging the initial, y_I, and final, y_F, traverse values of y_ℓ.

$$y_t = (y_I + y_F)/2 \tag{14}$$

The average bed slope, S_b, and watersurface slope S_w were obtained by averaging the initial and final traverse regression trends. The mean concentration from the density cell records was determined by subtracting the average of the initial and final traverse averages from the temporal average.

$$C_i = C_{iT} - (C_{iI} + C_{iF})/2 \tag{15}$$

Here C_{iI} and C_{iF} represent the apparent concentrations for the voltage output of the density cell/amplifier system for sediment-free water (measured during the initial and final traverses, respectively). This corrects C_{iT} for the zero level and compensates for any linear zero drift of the density cells during the temporal record period.

The discharge, Q_i, for each pump, i, was determined from the average pressure heads, h_i, by

$$Q_i = K_i[h_{iT} - (h_{iI} + h_{iF})]^{1/2} \tag{16}$$

where the subscripts T, I, and F denote temporal, initial spatial, and final spatial records, respectively and the K_i are the calibration factors of the elbow meters. The total flow discharge, Q, was then the sum of the individual pump discharges

$$Q = \sum_{i=1}^{3} Q_i \tag{17}$$

The average sediment concentration for the test channel was found by discharge-weighting the concentrations from each pump:

$$C = \sum_{i=1}^{3} C_i Q_i / Q \tag{18}$$

From the basic variables of the preceeding discussion (C, Q, y_t, S_w, and S_b), the sediment properties, and water temperature, all the basic variable relationships and similitude parameters suggested by the literature review could be determined. The mean velocity for the flow, V, was given by $Q/9y_t$ in ft. per sec. where the channel width is 9 feet. The Froude number, Reynolds number, and grain diameter similitude number were computed by

$$F = V/\sqrt{gy_t} \tag{19}$$

$$N_R = Vy_T/\nu \tag{20}$$

$$D = g^{1/3} d_{50}/\nu^{2/3} \tag{21}$$

To account for small differences in the average bed and watersurface slopes, the energy gradient, S_e, was computed by

$$S_e = S_w - F^2(S_w - S_b) \tag{22}$$

The energy gradient should be the best slope estimate for use in shear stress calculations, since it represents the average rate of change of the energy head per unit of channel length.

In addition to the mean values of the data records, the initial analysis program gave the standard deviations of the various record segments. Averages of the individual-record standard deviations could be determined by applying the appropriate calibration factors to the voltage standard deviations and averaging corresponding values. This procedure gave the spatial standard deviation of the bed surface, σ_{bL}; the temporal standard deviation of the bed surface, σ_{bt}; and the standard deviation of the concentration from each pump, σ_{ci}. Fluctuations of the pressure head from the discharge meters were assumed to be due to turbulent eddies in the pipe elbow rather than indications of actual discharge changes. Therefore, the composite concentration standard deviation was determined by discharge weighting the σ_{ci} values:

$$\sigma_c = \sum_{i=1}^{3} (\sigma_{ci}\, Q_i)/Q \tag{23}$$

Note should be made that these σ_c values are indicative of fluctuations in the concentration returned to the test channel and may not represent temporal fluctuations under equilibrium conditions in the channel itself or the discharge from the main channel into the return channel. The long return channel, highly complex flow patterns in the sump, and different locations of the three pumps relative to the sump inflow would be expected to modify the statistical properties of the concentration fluctuations.

Standard deviations of the data records serve as a measure of the relative magnitudes of the deviations from the mean, however they give no insight into the distributions of the fluctuations and time and spatial scales of the deviations. Both the dune amplitude and spatial distribution are assumed to influence flow resistance. A combination of their spatial and temporal distributions is necessary to assess the significance of the mean values of a data record. Little confidence could be placed in mean parameters of a data record that includes only one or two major cyclic periods (only one or two large dunes).

4.3 PROBABILITY DISTRIBUTIONS

To provide information on the relative distribution of the magnitudes of the deviations from the mean, the probability density function was chosen.

Time and length scales of the deviations were assumed to be defined by the spectral density functions. The mean of these functions (first spectral moments) defines the mean temporal and spectral frequencies which could be taken to represent the reciprocals of the mean scales of the bed forms or concentration distributions.

The probability density function (PDF) is determined in a straight - forward way. The precedure is to define the cumulative distribution (CDF) of the normalized data record and numerically differentiate it to obtain the PDF. For each of the data records the CDF was obtained by counting the number of normalized data values less than a series of specified levels (0.1σ increments) and dividing these counts by the total number of data values. The PDF is then found by differentiating the CDF or,

$$PDF(\sigma_j) = \frac{d\ CDF(\sigma_j)}{d\sigma_j} \tag{24}$$

where σ_j is the normalized standard deviation. The numerical approximation of this expression is

$$PDF(\sigma_j) = \frac{CDF(\sigma_{j+1}) - CDF(\sigma_{j-1})}{\sigma_{j+1} - \sigma_{j-1}} \tag{25}$$

The denominator of this expression is 0.2 for a σ increment of 0.1.

4.4 SPECTRAL CALCULATIONS

The method of Willis (1976), which will be summarized subsequently, for computing the dune load requires the spectral density and cross-spectral phase angles from dual records of bed elevation. These records must be from points ~~reported~~ separated some distance in the direction of dune migration. Calculations of the spectra and phase angles can be made from Fourier transforms of the cross-correlation function of the two records; however, this procedure is extremely slow requiring much computer time. To facilitate the calculations, a symmetrical-range Fast Fourier Transform

(FFT) algorithm was developed. The mathematical details of the FFT procedure will be omitted here because of its complexity. A manuscript presenting the development of the procedure has been submitted to the ASCE Journal of the Engineering Mechanics Division. Use of the spectral estimates from the bed-elevation data is summarized in the discussion that follows.

From previous work (Willis 1976) the volumetric dune load, G_d, is given by

$$G_d = \sqrt{2}\,\sigma_b \int_o^{fc} \frac{V(f)\,S(f)\,df}{2\left(\int_o^f S(f)df\right)^{1/2}} \tag{26}$$

where (f) is the frequency, V(f) is the migration velocity of the frequency component f of the data record, and S(f) is the spectral density (normalized by σ_b).

The symmetrical FFT algorithm was designed to compute the cross spectial density function for two records. The cross spectral density, SC(f) is a complex quantity that is expressed in terms of its symmetrical, C(f), and assymetrical, Q(f), parts as

$$SC(f) = C(f) - i\,Q(f) \tag{27}$$

or

$$SC(f) = |(SC(f))|\,e^{-i\theta(f)} \tag{28}$$

where θ is the phase angle between the wave components of frequency f from the two records. The magnitude of (SC(f)) is given by

$$|SC(f)| = [C(f)^2 + Q(f)^2]^{1/2} \tag{29}$$

Furthermore SC(f) can be shown to be

$$|SC(f)| = (S_1(f) \times S_2(f))^{1/2} \tag{30}$$

but since the two records of bed elevation are statistically the same

$$S_1(f) = S_2(f) = S(f) \tag{31}$$

and

$$|SC(f)| = S(f) \tag{32}$$

so that $|SC(f)|$ is used in lieu of $S(f)$ in the dune load equation.

The quantity $\theta(f)$ is the angle by which the f components of the two records are out of phase also, $\theta(f)/2\pi$ is the fraction of a period by which the f components are out of phase or the fraction of a period required for the f component to travel between the two ultrasonic probes. Provided that not more than one period elapsed between the transducers, the time lag is given by $\theta(f)/2\pi f$ and the velocity $V(f)$ by:

$$V(f) = \frac{2\pi\Delta x f}{\theta(f)} \tag{33}$$

where Δx is the transducer spacing. If more than one period elapses the quantity $\theta(f)/2\pi$ must be increased by the number of whole periods as determined by the number of times the phase angle swept through zero between 0 and f.

The phase angle $\theta(f)$ is calculated by

$$\theta(f) = \text{Arctan } (Q(f)/C(f)) \tag{34}$$

Thus the spectral calculations permit the dune load to be calculated. Other simplified approaches involve determining the time shift required to place the bed elevation records in phase, Υ, and defining a mean dune velocity, V_d, by:

$$V_d = \frac{\Delta x}{\Upsilon} \tag{35}$$

Other methods involve the spectral moments

$$\bar{f} = \int_o^{fc} fS(f)df \tag{36}$$

where $\bar{f}$ is the first spectral moment or mean frequency and

$$\overline{f^2} = \int_o^{fc} f^2 S(f)df \tag{37}$$

where $\sqrt{\overline{f^2}}$ is the second spectral moment or $\overline{f^2}$ is the mean squared frequency. Strictly from dimensional considerations, three other measures

of the dune velocity can be obtained from corresponding temporal and spatial frequency moments. The first is

$$V_d = \bar{f}_t / \bar{f}_L \tag{38}$$

where the subscript "t" denotes moments from the spectral analyses of the temporal records of bed elevation and "L" from corresponding analyses of the spatial bed-elevation records. Other estimates involving second moments are

$$V_d = (\overline{f_t^2} / \overline{f_L^2})^{1/2} \tag{39}$$

and

$$V_d = (\overline{f_t^2})^{1/2} / f_L \tag{40}$$

For either of these mean dune velocity estimates some estimate of the effective dune amplitude must be made to estimate dune load. Calculations of the standard deviations for regular wave forms show that the amplitude is $\sqrt{2}\sigma_b$ for a sinusoidal wave form, and $\sqrt{3}\sigma_b$ for a triangular wave. In view of the uncertainties concerning the estimates V_d as true measures of the dune velocity and since dunes are apparently composed of a combination of triangular and sinusoidal components, the 20 percent deviation in the amplitude estimate could probably be tolerated.

5 RESULTS

5.1 BASIC CORRELATIONS

Experiments were conducted in the 250-ft. test channel for three discharges with nominal values of 50, 100, and 150 cfs. For each discharge a series of flow depths were imposed by different positions of the tailgate. Assuming that influences of temperature were negligible, the other flow and transport variables would have adjusted in response to these controls. Any data relationship involving the other variables must be manifest in correlation between the variable of interest and the independent controls of discharge Q, or unit-width discharge q, and depth y_t.

Preliminary application of the analyses described in the previous section enabled us to evaluate the mean sediment concentration C, the standard deviation of the bed surface, σ_b, for both spatial and temporal records, the energy gradient, S_e, and the standard deviation of the concentration fluctuations. These quantities are presented in Table 1 and their various correlations with q and y_t are indicated in Figures 3-6. The various quantities are plotted against y_t with q as a parameter.

For three of the tests that were conducted stream monitor failure resulted in loss of both spatial traverse records, hence no depth determination could be made. No data comparison can be made for these tests. Where possible the reported depths and slopes are averages of those for the initial and final traverses. For a few of the tests the depth and slope are based on only one traverse because of failure of one of the stream monitor channels of the other traverse.

The best of the basic data correlations presented is apparently for σ_L, the spatial standard deviation of the bed elevation records. The bed standard deviation increases with increasing depth with an apparent single relationship right through the different discharges. As far as this correlation is concerned, an increase in discharge just increased the depth.

The relationship for the temporal standard deviation of the bed surface is not as good as that for the spatial records. A re-examination of the raw data showed that fewer bed form periods than wave lengths were represented in the data records. Hence, the precision of determining σ_t is not as good as that for σ_L. The temporal standard deviations are, on the

Table M.1: Basic Data

Test #	Temp. °F	Q_t cfs	y_t ft.	V ft./sec.	F	S_e x10^{-3}	$\bar{C}$ ppt	σ_L ft.	σ_t ft.
1		47.5156	2.2138	2.3848	0.2826	2.67673	0.8616	0.2493	0.2705
2		46.8944	2.0670	2.5208	0.3091	2.62478	0.6911	0.2652	0.2659
3		Data Lost							
4		47.0089	1.6408	3.1833	0.4382	2.12713	2.1490	0.1590	0.1000
5		45.4262	1.2631	3.9960	0.6269	3.05205	2.5703	0.0672	0.0780
6		45.0812	1.3361	3.7490	0.5718	3.87520	4.3947	0.0645	0.0705
7		46.2553	1.2572	4.0880	0.6428	3.22928	3.4674	0.0470	
8		Data Lost							
9		50.9808	2.2009	2.5737	0.3059	1.99382	1.3717	0.2715	0.2328
10	83°	51.1696	2.3642	2.4048	0.2757	1.26207	0.3684	0.2022	0.1532
11		50.3271	2.7077	2.0652	0.2213	0.57451	0.1910	0.1862	0.0617
12		Data No Good							
13	87°	51.4403	1.6943	3.3734	0.4569	3.27959	2.0008	0.1990	0.1986
14	89°	51.1113	1.5507	3.6622	0.5185	3.00451	2.3803	0.1825	0.1384
15	85°	101.5603	2.7197	4.1492	0.4436	2.40553	0.9186	0.2892	0.3247
16	86°	102.7748	2.7188	4.2002	0.4491	1.98201	0.6272	0.3538	0.3221
17	86°	100.3154	2.1129	5.2753	0.6399	3.20034	1.6700	0.2043	0.1231
18	86.5°	102.3126	2.4888	4.5677	0.5105	3.43646	0.9161	0.2804	0.2431
19	83°	93.9019	2.9136	3.5810	0.3699	2.47076	0.9265	0.2464	0.3363
20	83°	104.0262	3.5977	3.2127	0.2986	1.39368	0.6300	0.2965	0.3251
21	79°	100.8530	4.1044	2.7302	0.2376	0.66141	0.2045	0.2417	0.1608
22		Data No Good							
23	84°	152.2884	3.3696	5.0216	0.4823	3.60860	1.0653	0.4177	0.4132
24	78°	152.4664	3.6666	4.6203	0.4254	2.78209	1.2168	0.4603	0.4785
25	72°	153.1377	4.0099	4.2433	0.3736	1.84114	0.6448	0.3960	0.5105
26	68°	149.7231	4.4880	3.7068	0.3085	1.51062	0.9116	0.3924	0.4265
27	70°	149.9670	4.6293	3.5995	0.2950	1.60742	0.7966	0.3695	0.4241
28	64°	149.0660	3.7203	4.4520	0.4070	2.08974	1.1100	0.3710	0.5018
29		Data No Good							
30	54°	149.7831	4.3012	3.8693	0.3289	2.36413	0.8643	0.5061	0.5003
31	59°	144.2571	3.8974	4.1126	0.3673	2.53624	0.8345	0.4268	0.6216

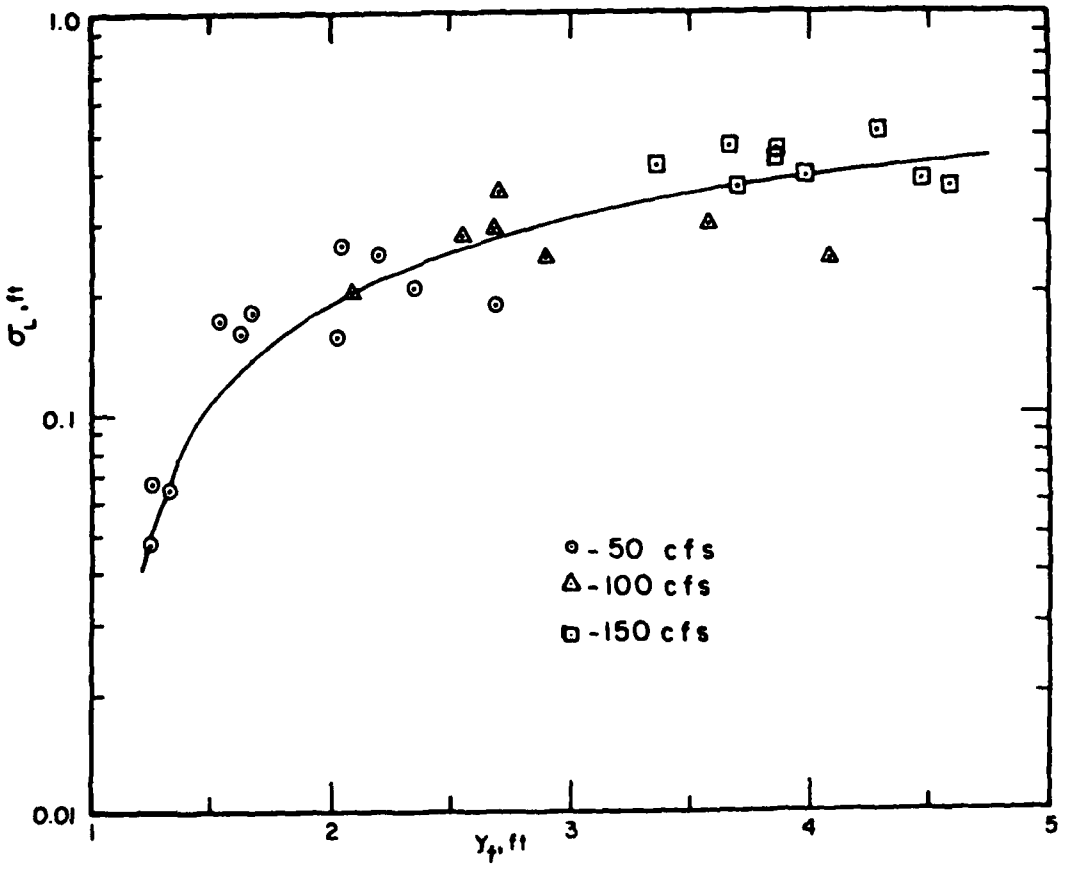

Fig. 3: Standard Deviations of Spatial Bed Elevations

average, slightly smaller than the spatial standard deviations. This is probably due to a biased estimate of the mean trend of the temporal data through inclusion of too few dune periods. The standard deviations are computed for deviations from the mean trend and the trend would be biased also for too few periods. In particular, the two data points falling much below the others in Figure 4 are for tests nos. 11 and 21 for which the temporal data included no more than one dune. For tests 25 through 31 the temporal record period was extended to about 6 hours to include more dune periods. Even this length of record would be inadequate for the slowly moving dunes of low transport tests.

The correlation that is of primary interest in this project is that for total concentration of bed material. Figure 5 presents this basic variable relationship. Although the scatter is typical of that for concentration measurements, definite trends are apparent. Concentration decreases for increasing depth for a constant discharge, however, the change in concentration for a 1.5 ft. change in depth is much less for the 150-cfs tests than for the 50-cfs tests.

The energy gradient depicts a similar type correlation as shown in Fig. 6 except that the range of energy gradients was about the same for each of the discharges. Decrease in energy gradient with increasing depth at a given discharge and increase in energy gradient with increasing discharge at the same depth is qualitatively consistent with expected trends.

These basic correlations serve primarily to indicate the ranges and precision of determination of the various variables. They do not represent general relationships that would be applicable to another set of conditions unless the same magnitudes of the variables were reproduced. This would be very restrictive in that no information for flows over 16.7 cfs per foot of channel width are represented in the graphs.

5.2 SIMILITUDE RELATIONSHIPS

Similitude relationships are a means by which experimental results are presented in a format that is independent of the scale of the flow system. Of course complete similitude can seldom be achieved, so one of the primary goals of this investigation was to test the similitude relationships that have been defined by smaller-scale investigations. If the results of the small-scale investigations reliably model the larger scale flows of this

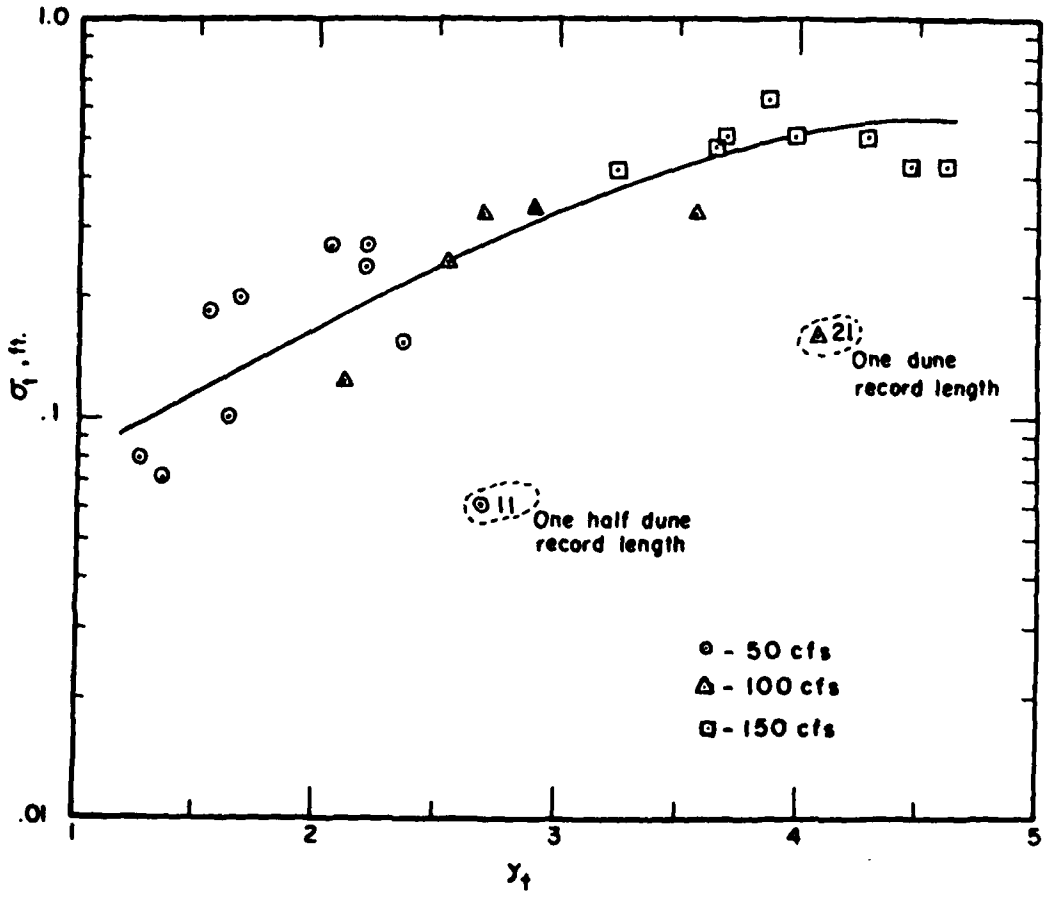

Fig. 4: Standard Deviations of Temporal Bed Elevations

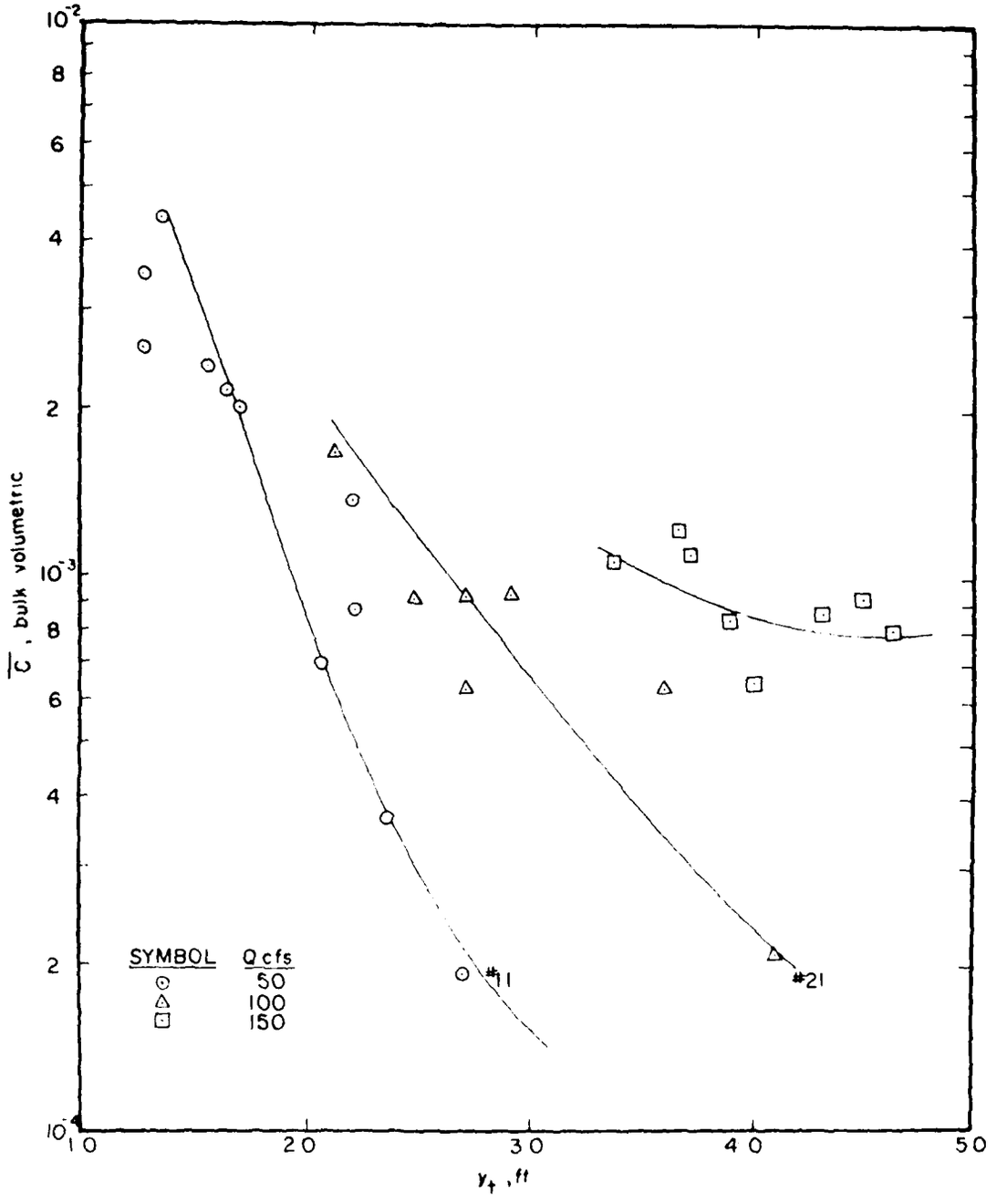

Fig. 5: Concentration as a Function of Depth and Discharge

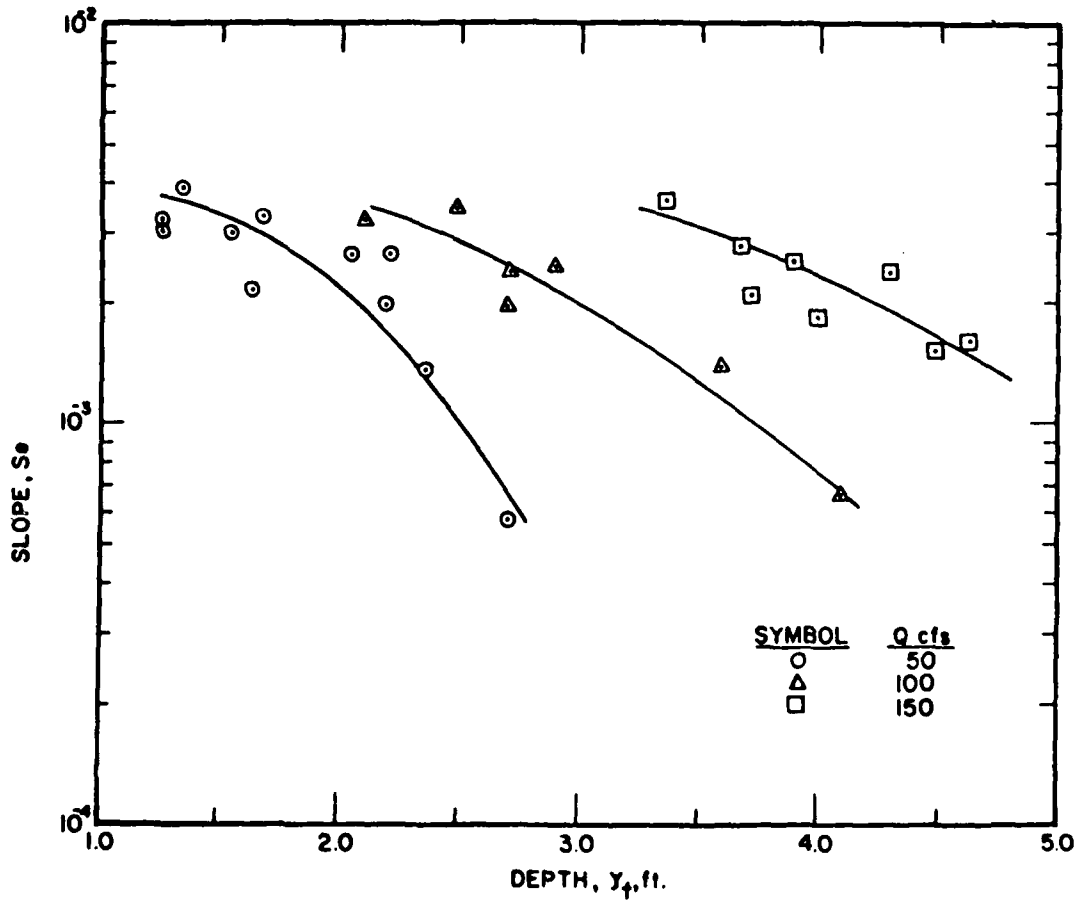

Fig. 6: Energy Gradient vs. Depth and Discharge

investigation, more confidence is obtained in extending them to still larger flows. Similitude theory suggests that dimensionless expressions of the various dependent variables may depend on both the Reynolds number and the Froude number, which are dimensionless expressions of the unit width discharge and depth.

Viscous influences in hydraulics are usually negligible at high Reynolds numbers with the various quantities correlating well with Froude numbers alone. Application of the Froude number relationships to larger flows (higher Reynolds numbers) is contingent upon independence of the Reynolds number.

Figure 7 presents the correlation of the total discharge concentration from the density cell as a function of Froude number. The average line from small-scaled tests (Willis, 1974) with the same average grain diameter similitude number, D = 14.0, is superimposed thereon. Here

$$D = d_{50}\, g^{1/3}/\nu^{2/3} \tag{41}$$

The three nominal discharges have Reynolds numbers of 5×10^6, 1×10^7, and 1.5×10^7. Tests with N_R values near these are coded with different symbols. Data from Guy, et al. (1966) for about the same size sediment (0.54 mm) in a 2-ft. wide test channel are also included for comparison. These data were dominant in establishing the curve, Willis (1974).

Concentrations from the 250-ft. flume were significantly higher than those from small scaled tests for the same Froude number. Although data are not adequate to resolve any Reynolds number dependency between 0.5×10^7 and 1.5×10^7, the curve shift may be a Reynolds number effect, the similitude number D may not adequately specify grain diameter similitude, or data from small flume experiments for this sediment size may not be general. A change in the length scale for a given Froude number gives a velocity scale proportional to the square root of the length scale. If this same velocity scale is applicable to the vertical velocity fluctuations from turbulence and the captive eddy on the lee slopes of dunes, then the sediment particle fall velocity should be adjusted accordingly. A constant D value would give the same fall velocity for different scaler. Hence, the data from these large-scale tests would be more nearly comparable with the results from smaller flumes with finer sediments. However, the data from Stein (1965) for 0.4 mm sand also gives lower concentrations. The greater velocity fluctuations from larger scale

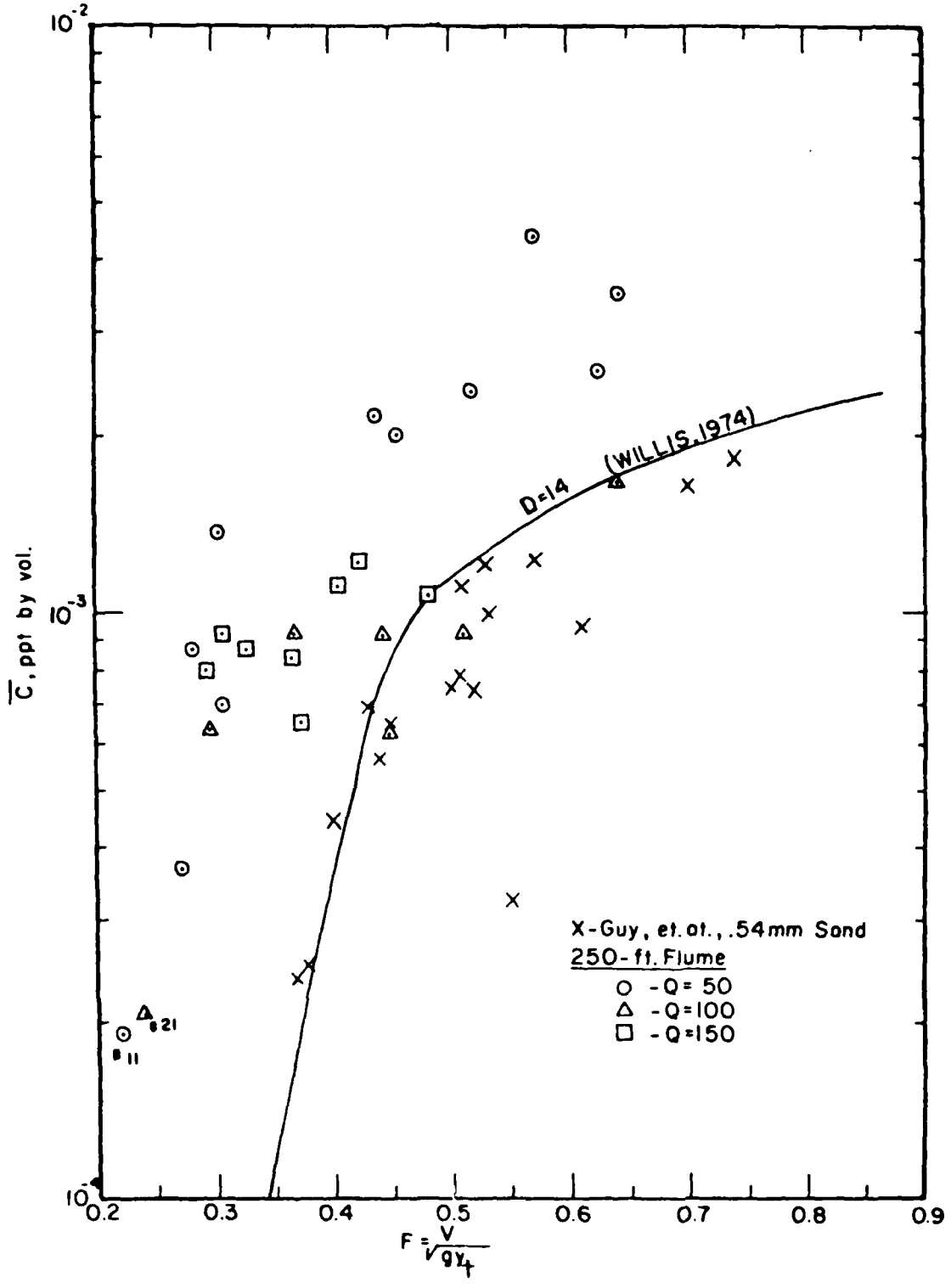

Fig. 7: Sediment Concentration vs. Froude Number

systems would result in greater upward diffusion of sediment and a greater bed material load of a given sediment size. However, this does not require that the dimensionless load (concentration) be higher.

The mechanics of applying a fall velocity correction in view of the fact that an experimental investigation encompasses a range of depths (length scales) is not immediately evident. Also, data from smaller flumes do not suggest an increase in sediment concentration with decreasing particle size of a magnitude comparable to that indicated by these data. Thus, the increased transport capacity of the large-scale tests is an unexpected result and represents a definite need for future research.

One of the requirements of similitude is that the flow systems be geometrically similar. This implies that the bed geometry with respect to other scales such as the depth should bear the same relationship with Froude number. The standard deviation of the bed surface (σ_b) was chosen as a measure of the dune heights; the relation of σ_b with Froude number for both spatial and temporal bed-elevation records is shown in Figs. 8 and 9. Average curves from previous work are included for comparison.

Relative to the flow depth the standard deviations were of about the same order of magnitude for the large and small-scale results. Hence the bed configurations were geometrically similar. The graph of σ_L/y_t in Fig. 8 suggests a shift of the curve to lower Froude numbers for the large scale data. This same trend is also apparent for concentration data. In fact, a 35-40 percent reduction in the Froude number of the relationships for smaller flumes would give a much better fit of the data from this investigation. This would suggest that scale adjustments might be accomplished by a change in the index Froude number relationship of Willis (1974). However until more experimental data are available, only conjectures can be offered to explain or account for the differences between results from the different scale tests.

The energy gradient is dimensionless and independent of the scale of the flow system for total similarity. The three curves of Fig. 6 do indeed collapse into one in terms of the Froude number as shown in Fig. 10. These data indicate an increasing energy gradient with Froude number. Although Fig. 10 represents a resistance relationship for the test channel, it is customarily represented in terms of a resistance factor such as the Darcy-Weisbach friction factor f. By definition, f is determined by:

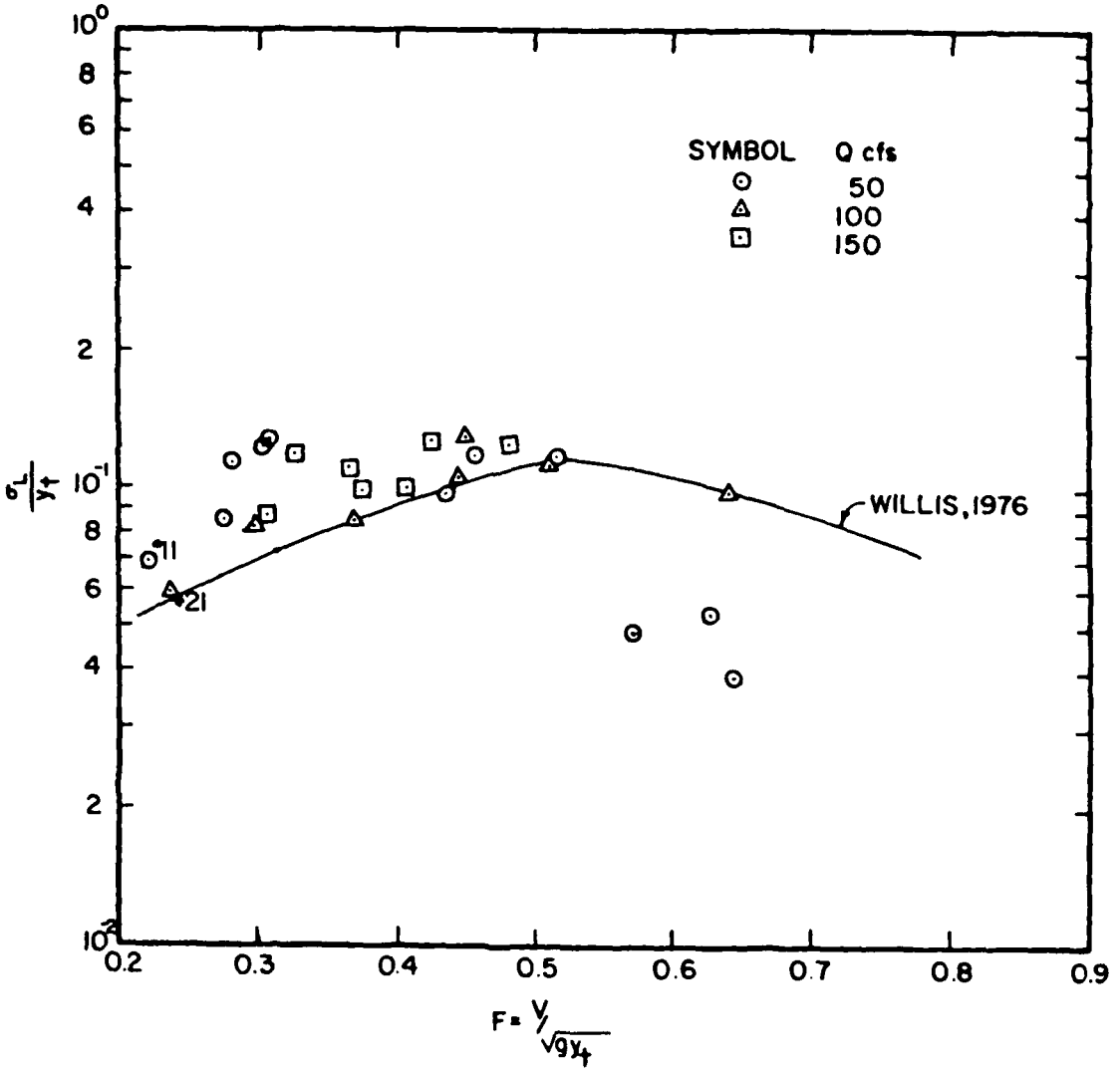

Fig. 8: Relative Spatial Standard Deviation of Bed Forms

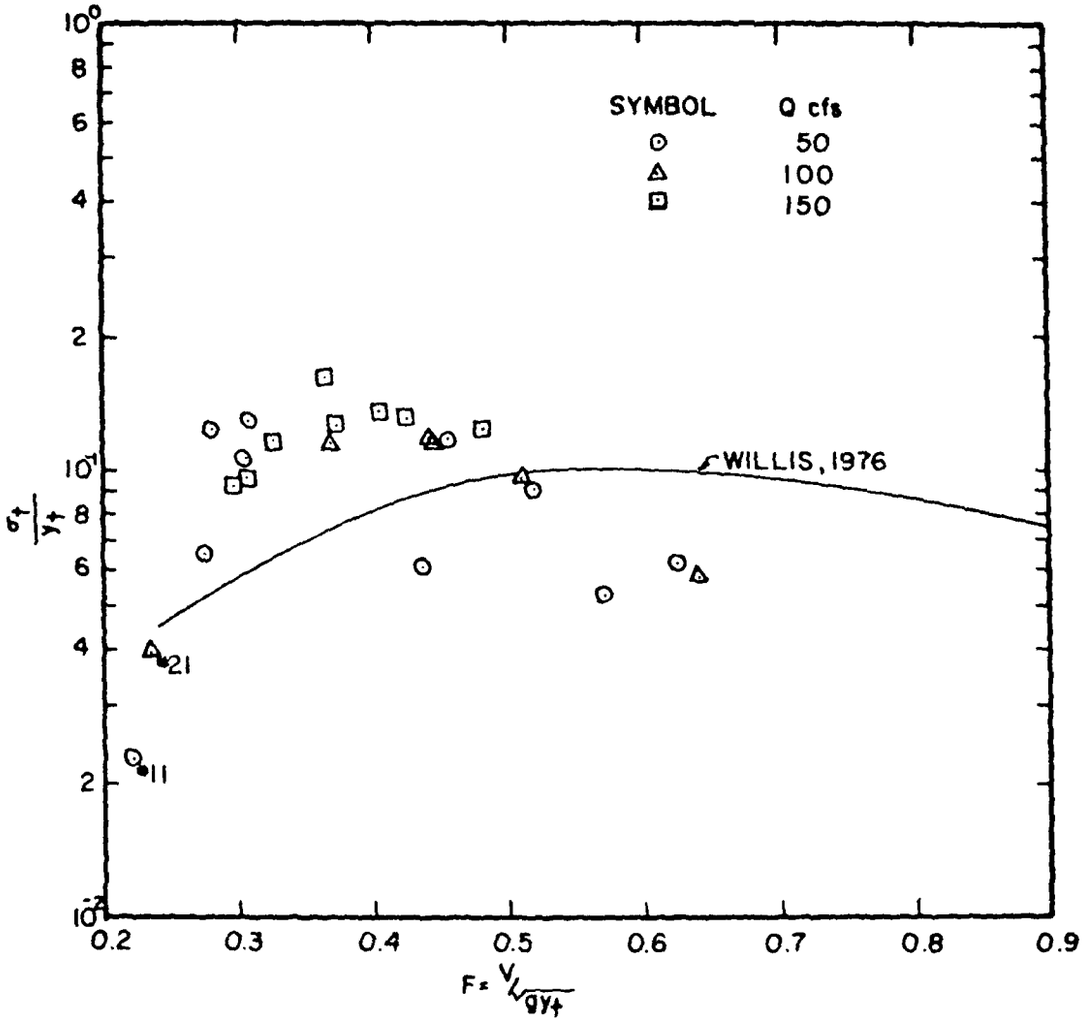

Fig. 9: Relative Temporal Standard Deviation of Bed Forms

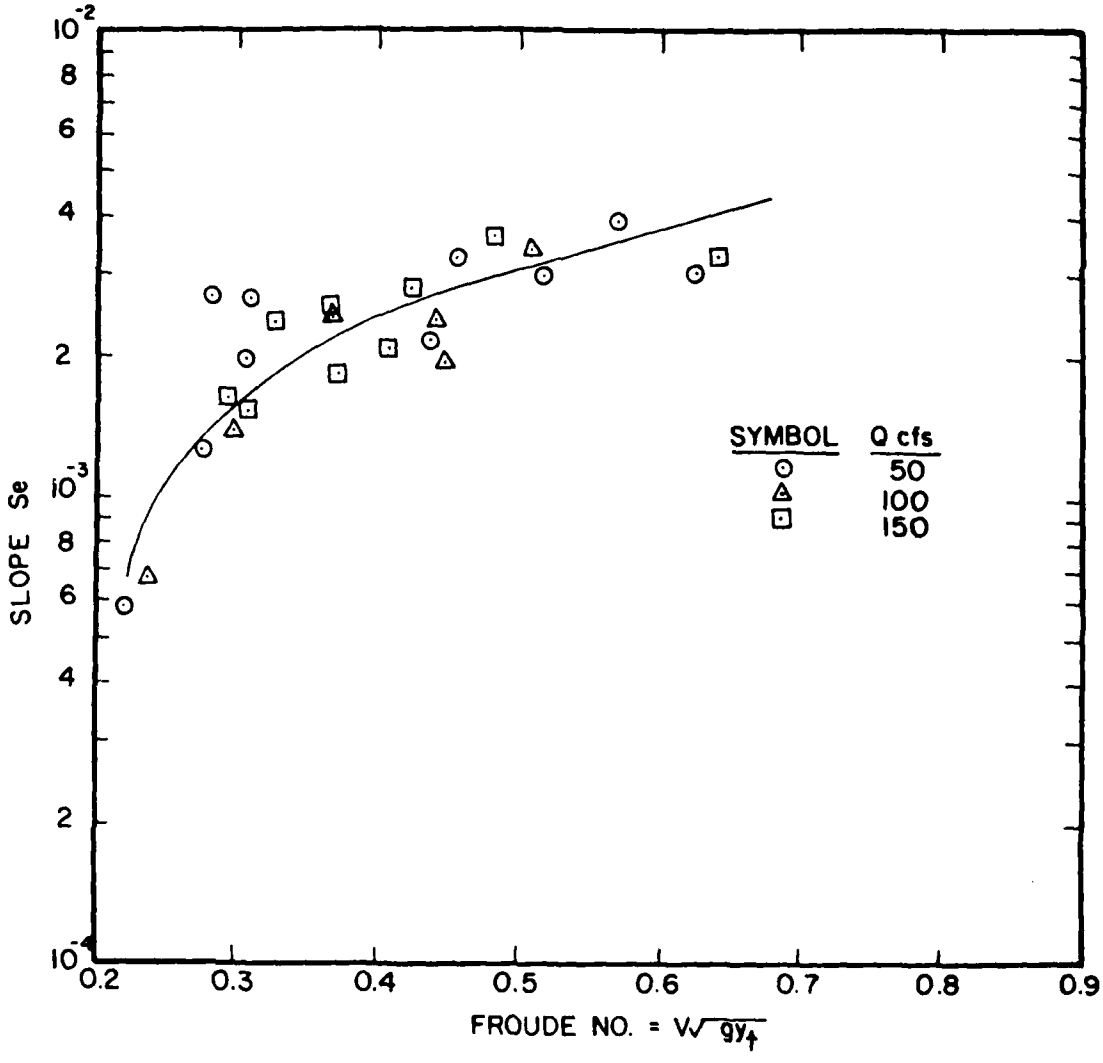

Fig. 10: Energy Gradient as a Function of Froude No.

$$f = 8\ S_e/F^2 \tag{42}$$

Since F^2 is already considered as the independent parameter, no new generalities are obtained from the f relationship over that for S_e; however, for consistency with previous work the f vs. F relationship is depicted in Fig. 11. The friction factor apparently reaches a maximum value at a Froude number of about 0.3 corresponding roughly to the lower Froude number of the highest relative roughness of the bed surface.

The report of the ASCE Task Committee (1971) suggests that different curves should be depicted for the different depths of flow in Figure 10. Thus the appearance of a single-curve relationship for these data may be an artifact of the particular depth range that was encountered in the experiments.

5.3 SPECTRAL RELATIONSHIPS

The Fourier spectra and frequency moments of the temporal and spatial bed elevation records were computed. The usual spectral moments were computed by:

$$f^n_{mean} = \int_0^1 f^n\, d\sigma^2 \tag{43a}$$

$$= \int_0^{f_c} f^n\, S(f)\, df \tag{43b}$$

where n denotes the order of the moment and f_c is the cutoff frequency.

The dune load from equation (26) represents the product of an effective dune amplitude, $\sqrt{2}\ \sigma_b$, and an average dune velocity, relative to contributions from various spectral components to the standard deviation of the bed surface; ie,

$$V_{d_{average}} = \int_0^1 V(f)\, d\sigma \tag{44a}$$

$$= \int_0^{f_c} \frac{V(f)S(f)\, df}{2\sigma} \tag{44b}$$

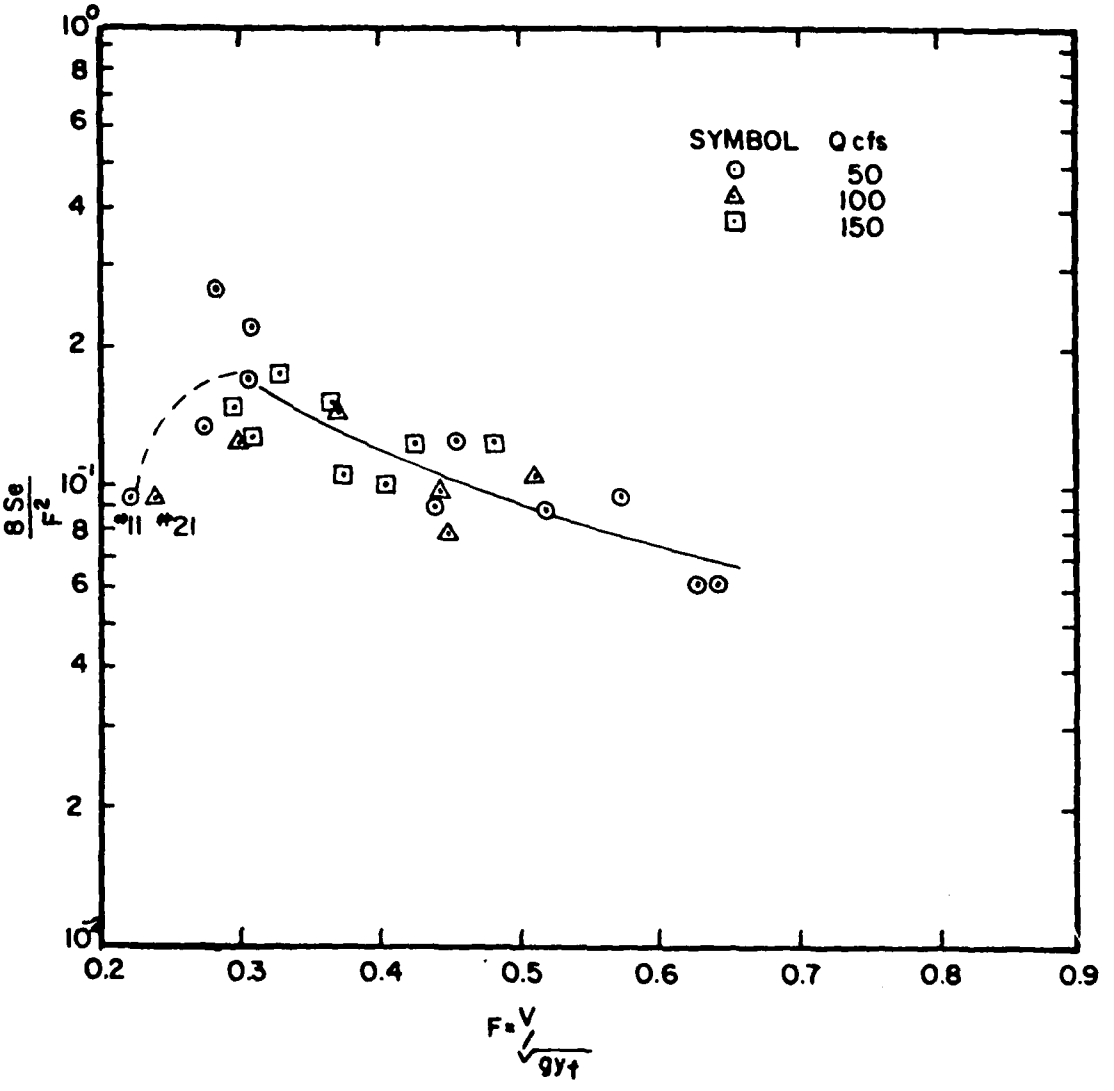

Fig. 11: Friction Factor as a Function of Froude No.

Since the $d\sigma$ contributions influence the sediment load directly, other frequency moments were similarly defined.

$$f^n_{average} = \int_0^1 f^n \, d\sigma \tag{45a}$$

$$= \int_0^{f_c} \frac{f^n \, S(f) \, df}{2\sigma} \tag{45b}$$

Recriprocals of mean frequencies are usually taken to approximate the mean periods or wave lengths, however averages of the individual-component wave lengths (n = -1 in eqns. 43 and 45) were included in the analysis programs. The various moment calculations are presented in Table 2. The "mean" values denote the averages with respect to the spectral or variance contributions (Eqns. 43). The "average" values denote the averages with respect to the standard deviation contributions (Eqns. 45).

The scatter of the various spectral estimates is too great to establish definative relationships and permits only general trends to be deduced from the data. Correlations involving the mean and average periods and wave lengths exhibited somewhat less scatter than those for the frequencies. Also, the average values were slightly more consistent than the mean values. This is probably due to the fact that the periods and wave lengths are dominated by the low-frequency components. Erratic high-frequency components may have been contributed by loss of ultrasonic signals and/or reflections from clouds of suspended sediment near the bed.

Figure 12 presents the average wave length, normalized by flow depth, as a function of the squared Froude number. The data for tests at 50 cfs exhibit longer average wave lengths relative to the flow depth than those for the two higher flow rates. The longer wave lengths also tend to persist for higher Froude numbers than they did for small-scale flows. This tends to cast doubt on the geometric simularity of bed forms for different scale flow systems, but it may also suggest that the large test channel was not long enough to establish equilibrium wave lengths for such large dunes.

The average period is shown, versus Froude number, in Fig. 13. Although the data scatter appreciably, a trend of decreasing period with increasing Froude number is apparent. The average period is large thus it

Table M.2: Bed-Form Frequency Estimates

Test No.	F	Spatial					Temporal				
		Averages		Means			Averages		Means		
		f_L	L Wave Lgth.	f_L	L Wave Lgth.	$\sqrt{f_L^2}$	f_t	T Period	f_t	T Period	$\sqrt{f_t^2}$
		cycles/ft	ft	cpf	ft	cycles/ft	cps	sec	cps	sec	cps
1	0.283	0.0594	19.12	0.0801	13.25	0.151	0.000784	2263.	0.000130	2689.	0.0122
2	0.309	0.0715	14.88	0.0956	10.71	0.194	0.000931	3303.	0.00204	5256.	0.0149
3	Data Lost										
4	0.438	0.0501	20.04	0.0619	12.94	0.182	0.00677	1351.	0.0118	864.	0.0299
5	0.627	0.120	15.52	0.160	7.91	0.336	0.00934	901.	0.0170	463.	0.0356
6	0.572	0.133	19.07	0.207	12.05	0.385	0.00761	554.	0.0122	277.	0.0287
7	0.643	0.0580	17.41	0.0858	15.40	0.321					
8	Data Lost										
9	0.306	0.0936	18.24	0.143	13.69	0.279	0.00171	3043.	0.00365	4282.	0.0226
10	0.276	0.124	16.60	0.192	11.45	0.634	0.00447	1553.	0.00606	1135.	0.0272
11	0.221	0.140	13.88	0.210	8.98	0.683	0.01200	493.	0.0126	226.	0.0350
12	Data No Good										
13	0.457	0.106	21.03	0.175	16.67	0.696	0.00254	2206.	0.00520	2114.	0.0244
14	0.519	0.125	20.56	0.214	18.38	0.816	0.00381	1668.	0.00723	1292.	0.0272
15	0.444	0.144	21.99	0.256	18.51	0.833	0.00152	2773.	0.00297	3738.	0.0177
16	0.449	0.0926	14.14	0.120	8.77	0.632	0.00192	2394.	0.00356	2581.	0.0200
17	0.640	0.194	33.98	0.335	29.70	1.157	0.00745	1745.	0.0132	1408.	0.0347
18	0.511	0.197	22.29	0.294	25.58	1.119	0.00117	1811.	0.00175	1441.	0.0142
19	0.370	0.249	12.81	0.354	6.90	1.046	0.00543	1358.	0.00634	869.	0.0261
20	0.299	0.137	11.64	0.202	8.45	0.806	0.00177	1807.	0.00230	1530.	0.0184
21	0.238	0.144	13.81	0.210	8.28	0.884	0.00323	2297.	0.00537	2561.	0.0253
22	Data No Good										
23	0.482	0.0849	23.29	0.146	23.92	0.699	0.00132	2724.	0.00266	3375.	0.0178
24	0.425	0.0756	17.64	0.0986	12.14	0.586	0.00181	1245.	0.00199	694.	0.0158
25	0.374	0.0715	16.12	0.0911	10.52	0.518	0.000481	4029.	0.000738	2898.	0.00495
26	0.309	0.136	16.19	0.212	12.05	0.891	0.000859	4161	0.00153	3546.	0.00825
27	0.295	0.135	15.95	0.195	9.77	0.845	0.00127	3736.	0.00191	2291.	0.00878
28	0.407	0.217	15.57	0.341	10.33	1.040					
29	Data No Good										
30	0.329	0.139	14.21	0.198	9.58	0.909	0.000893	5115.	0.00169	4416.	0.00807
31	0.367	0.167	18.73	0.247	13.97	1.043	0.00161	1369.	0.00198	689.	0.00837

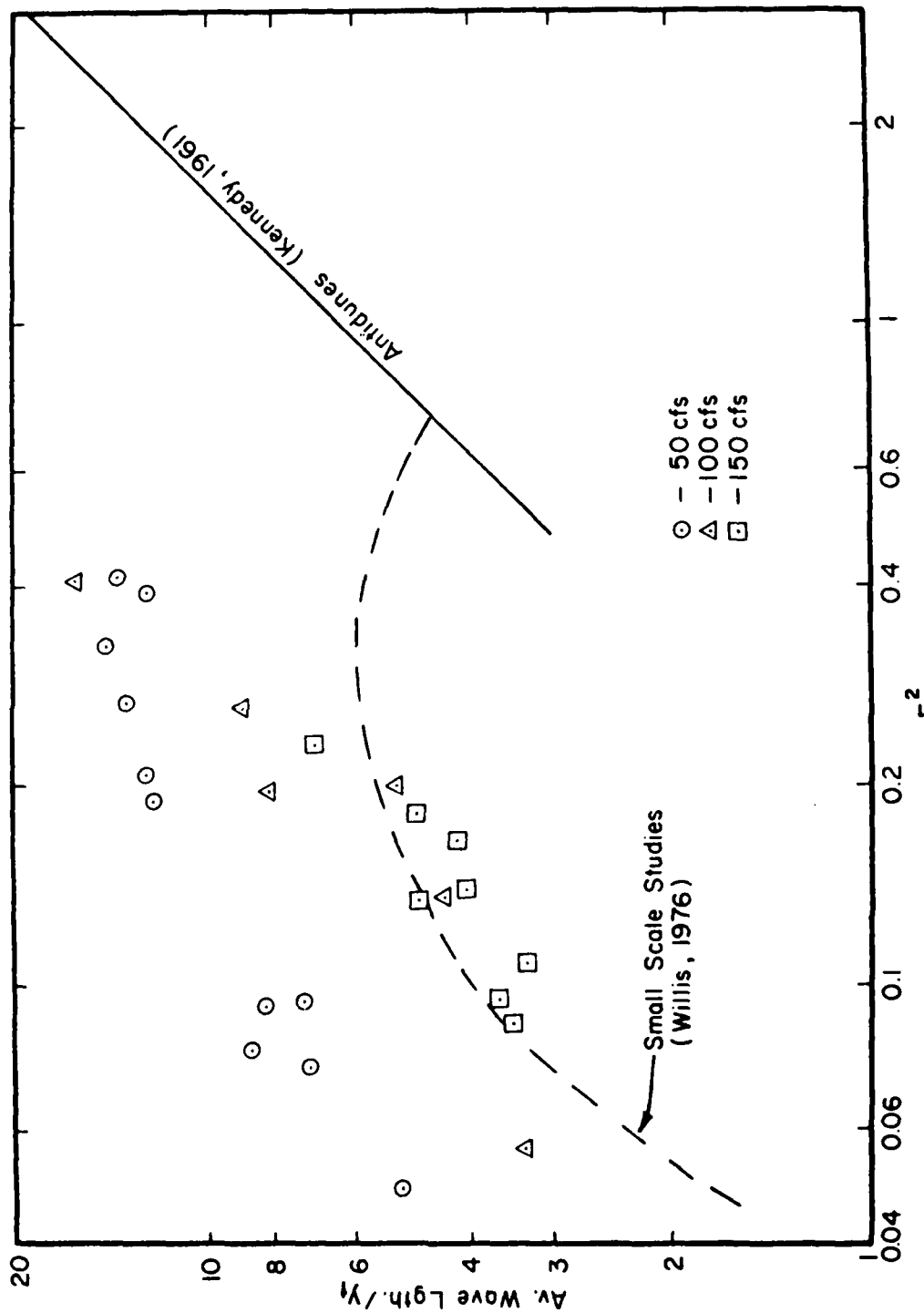

Fig. 12: Relative Wave Length of Bed Forms

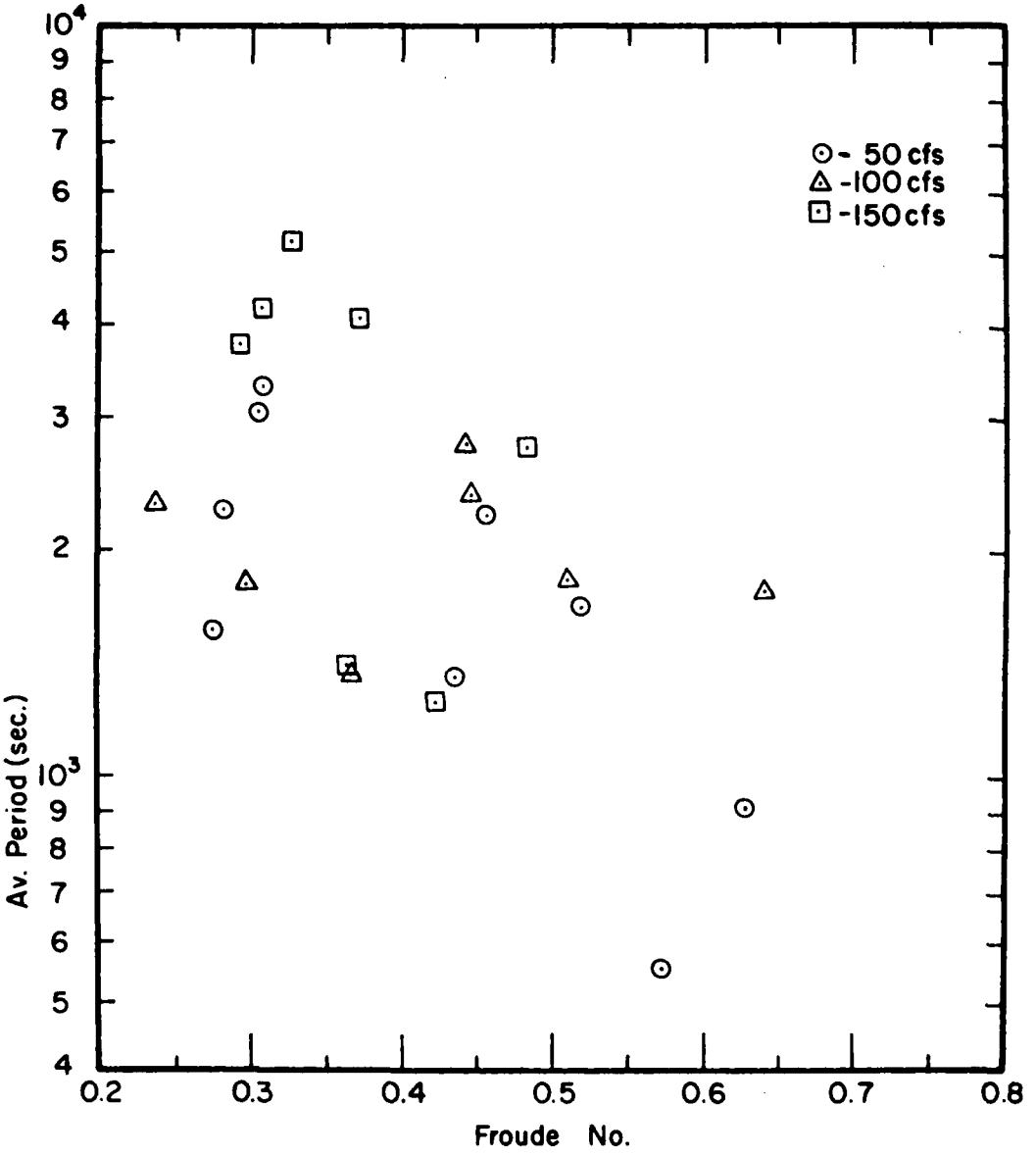

Fig. 13: Bed-Form Period

casts doubt on the validity of the temporal spectral estimates. The time of record for all but the last 6 tests was 8192 sec. For several of the tests, the record length included fewer than 5 periods and only one test encompassed over 10 periods. Hence, the degree of precision in estimating the average period as well as other temporal spectral parameters must be considered low.

Failure of one channel of the ultrasonic distance meter limited the estimates of individual component velocities and the average dune velocity by Eq. 44 to only seven tests. These estimates, along with others obtained by dividing the average wave length by the average period, are shown in Figure 14. The two estimate methods seem to be comparable and the dune velocity increases with increasing Froude number.

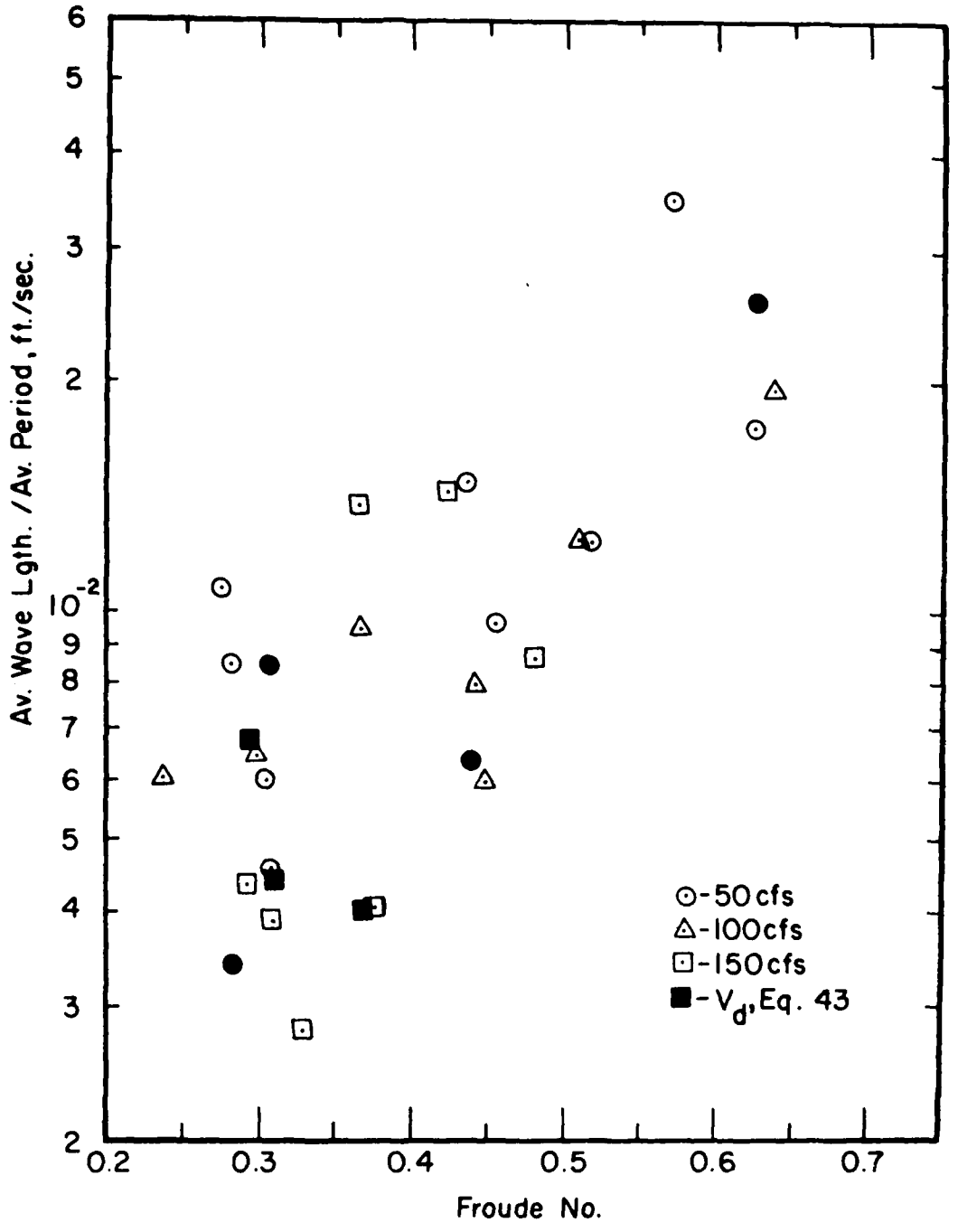

Fig. 14: Migration Velocity Estimates of Bed Forms

SUMMARY

In summary, the results of the large-scale flume studies indicate mean concentrations that are significantly larger than those for published small-scale studies for the same bed material size. The standard deviation of the bed surface relative to the flow depth was similar to that of small-scale tests, but the wave lengths were relatively longer over much of the Froude number range. The Froude number remains the primary independent flow similitude number controlling alluvial channel processes, but the question of sediment size similitude is yet to be resolved. The longer wave lengths relative to flow depth suggest similarity with coarser sediments, but the higher sediment concentrations are more consistent with finer sediments.

Temporal spectral calculations revealed dune periods that were not short relative to the length of record. Hence, the reliability of estimates based on the temporal records, including the mean concentration, should be considered low. An additional test series is planned to include longer temporal records encompassing at least 5 and preferably 10 dune periods.

Additional experimental work will be needed to explain the unexpected deviations of the data from the relationships defined by small-scale investigations. Until these deviations can be explained as artifacts of the particular investigations or accounted for by alternate methods of prescribing sediment-size similitude, the quest for a reliable, generally applicable sediment load predictor will not be finished.

REFERENCES

ASCE Task Committee, 1971, "Sediment Transportation Mechanics: Hydraulic Relations for Alluvial Streams," Journal of the Hydraulics Division, ASCE, Vol. 97, No. HY2, pp. 101-141.

ASCE Task Committee, 1971, "Sediment Transportation Mechanics:Sediment Discharge Formulas." Journal of the Hydraulics Div., ASCE, Vol. 97, No. HY4, pp 523-567.

Brown, Carl B., 1950, "Chapter XII, Sediment Transportation," Engineering Hydraulics, Hunter Rouse, Editor, John Wiley & Sons, Inc., New York, p. 794.

Colby, Bruce R., 1964, "Discharge of Sands and Mean Velocity Relationships in Sand-Bed Streams," USGS Prof. Paper 462-A, Washington, D.C., 47 p.

Coleman, N.L., 1969, "A New Examination of Sediment Suspenson in Open Channels," Journal of Hydraulic Research, Vol. 7, No. 1, pp. 67-82.

Crickmore, M.J., 1967, "Measurement of Sand Transport in Rivers with Special Reference to Tracer Methods," Sedimentology, Vol. 8, pp. 175-228.

Einstein, H.A., 1950, "The Bed-Load Function for Sediment Transportation in Open Channels," USDA, SCS Technical Bulletin 1026, Washington, D.C., 71 p.

Englund, Frank, 1966, "Hydraulic Resistance of Alluvial Streams," Jour. Hydr. Div., ASCE, Vol. 92, No. HY2, pp. 315-326.

Gilbert, G.K., 1914, The Transportation of Debris by Running Water, USGS Professional Paper 86, Washington, 263 p.

Hunt, J.N., 1954, "Turbulent Transport of Suspended Sediment in Open Channels," Proc. Royal Society of London, Series A, Vol. 224, No. 1158, pp. 322-335.

Lee, B. K., and Jobson, H. E., 1974, "Stochastic Analysis of Dune Bed Profiles," Jour. Hydraulics Div., ASCE, Vol. 100, No. HY7, pp. 849-867.

Nordin, C.F., Jr., 1971, "Statistical Properties of Dune Profiles," USGS Prof. Paper 562-F, Washington, 41 p.

O'Brien, M.P., 1933, "Review of the Theory of Turbulent Flow and its Relation to Sediment Transportation," Transactions, AGU. Vol. 14, pp. 487-491.

Rouse, Hunter, 1937, "Closure Discussion to 'Modern Conceptions of the Mechanics of Fluid Turbulence'," Transactions, ASCE, Vol. 102, pp. 523-543.

Rouse, Hunter, 1939, "Experiments on the Mechanics of Sediment Suspension," Proceedings Fifth International Congress of Applied Mechanics," Cambridge, Mass., pp. 550-554.

Shultz, Sam, 1968, and Hill, Ralph D., "Bedload Formulas," Hydraulics Laboratory Bulletin, Pennsylvania State Univ., 153 p. + part B.

Simons, D. B., 1965, Richardson, E.V., and Nordin, C.F., Jr., "Bedload Equation for Ripples and Dunes," USGS Prof. Paper 462-H, 9 p.

Squarer, D., 1970, "Friction Factors and Bed Forms in Fluvial Channels," Journal of the Hydraulic Div., ASCE, Vol. 96, No. HY4, pp. 995-1017.

Stein, Richard A., 1965, "Laboratory Studies of Total Load and Apparent Bed Load," Jour. Geophysical Research, Vol. 70, No. 8, pp 1831-1842.

Vanoni, Vito A., 1946, "Transportation of Suspended Sediment in Water," Transactions ASCE, Vol. III, pp 67-133.

Williams, G.P., 1970, "Flume Width and Depth Effects in Sediment - Transport Experiments," USGS Professional Paper 562-11, Washington, 37 p.

Willis, J.C., 1968, "A Lag-Deviation Method for Analyzing Channel Bed Forms," Jour. Hydraulic Research, Vol. 4, No. 6, pp. 1329-34.

Willis, Joe C., 1969, and Coleman, N. L., "Unification of Data on Sediment Transport in Flumes by Similitude Principles," Water Resources Research., Vol. 5, No. 6, pp 1330-1336.

Willis, J.C., 1971, "Erosion by Concentrated Flow," ARS 41-179, 16 p.

Willis, J. C., 1972, Coleman, N.L. and, Ellis, W.M., "Laboratory Studies of the Transport of Fine Sand," ASCE Journal of the Hydraulics Division, Vol. 98, No. HY3, pp. 489-501.

Willis, Joe C., 1976, "Sediment Discharge of Alluvial Streams Calculated From Bed-Form Statistics," Ph.D. Thesis, The University of Iowa, 200 p.

Willis, J. C., 1979, "Generalized Distribution of Turbulent Diffusivity," Journal of Hydraulic Research, Vol. 17, No. 3, pp. 231-250.

Willis, J.C., 1980, "Discussion of 'Spurious Correlation in Dimensional Analysis'," Journal of the Engineering Mechanics Division, ASCE, Vol. 106, No. EM6, pp. 1447-1456.

Yang, C.T., 1973, "Incipient Motion and Sediment Transport," Journal of the Hydraulics Div., ASCE, Vol. 99, No. Hy 10, pp. 1679-1704.

Zagustin, K., 1968, "Sediment Distribution in Turbulent Flow," Journal of Hydraulic Research, Vol. 6, No. 2, pp. 163-172.